Study on effective measures of power fluctuation mitigation for wind and solar power and electricity prices toward a predetermined social optimum

風力・太陽光発電の効果的な出力変動抑制対策と
社会最適誘導電力料金に関する研究

A dissertation submitted in partial fulfillment of the requirements for the degree of
Doctor of Philosophy in Engineering

By

LUKWESA BINESS

Division of Energy and Environmental Systems

Graduate School of Engineering, Hokkaido University, Japan

March 2023

Abstract

The development of variable renewable energy (VRE), which includes wind and solar photovoltaic (PV), is essential for reducing greenhouse gas (GHG) emissions and increasing energy security. The decline in the costs of VRE technologies, coupled with supporting policies such as a feed-in tariff (FIT) policy, has contributed to the rapid growth of VRE deployment. However, the integration of large-scale VRE poses a challenge to power supply systems due to fluctuations in VRE power output. Therefore, economical and technologically effective ways of integrating high shares of VRE into the power supply system need to be carefully considered. The effective integration of VRE in power supply systems should ensure that the effects of VRE power output fluctuations are minimized. The fluctuation reduction measures considered in this research include the geographical distribution of VRE locations, the introduction of battery storage, and the increase in power transmission capacity. This research investigates the effective combination of power fluctuation reduction measures toward optimum social costs of power supply. Further, the research employs a combined total and partial optimization approach to increase the utilization of VRE electricity in the power supply. The objectives of this research are: (i) to determine the effective combination of technological measures to suppress the VRE power output fluctuations and the increase in power supply costs when high VRE shares are integrated, and (ii) to elucidate the effective conditions of electricity prices required to achieve optimum VRE electricity utilization. This dissertation consists of 5 chapters as follows:

Chapter 1 summarizes the literature review and provides the objectives of the research.

Chapter 2 presents 2 linear programming-based optimization models which were developed for the analysis and a description of the case study area. The models include a total optimization and a partial optimization model. The total optimization model is employed to examine the effects of power fluctuation mitigation measures on the integration of large-scale VRE in power supply systems. The objective function is the total cost of power supply, which includes investment, operation and maintenance, and variable costs of power generation, energy storage, and power transmission systems. The model minimizes the total cost of the power supply. The partial optimization model is employed to optimize the power transmission and distribution (PTD) company. The objective function is the PTD company costs, which include the cost of electricity purchase and the cost of installation and maintenance of battery storage and power transmission systems. The partial optimization model minimizes the PTD company costs.

Chapter 3 is a study on effective measures for power fluctuation mitigation of geographically distributed wind and solar power. This study considers power fluctuation mitigation measures including the introduction of battery storage and an increase in the power transmission capacity. The study employs a total optimization approach to determine the effective combination of fluctuation reduction measures toward the minimized total cost of power supply. The results show that for high VRE shares, combining the geographical distribution of VRE locations with the introduction of battery storage and an increase in power transmission capacity effectively suppresses the increase in power supply cost. The variation of power supply costs and the VRE share can be categorized into three tiers. The first tier, up to 40 % VRE share, can be achieved by only optimizing the geographical distribution of the VRE locations. For the second tier of VRE share (40 % to 60 %), increasing the transmission capacity is effective to suppress the increase in the power supply cost and the excess power generation. In the third tier (60 % to 80 %), the effect of the introduction of battery storage is effective and is similar to the combined measures. Therefore, the selection of the appropriate measures for the integration of 60 % to 80 % VRE shares depends on government policies. The results also indicate that the introduction of battery storage facilitates the integration of large-scale solar PV while increasing the transmission capacity enables the integration of large-scale wind power. Further, in addition to battery storage and power transmission enhancement, a thermal energy backup system such as a combined heat and power (CHP) system may be effective in suppressing the increase in the total cost of power supply.

Chapter 4 is a study on electricity prices for power supply toward an optimum target of VRE electricity utilization. In chapter 3, a model of the entire power supply system is determined through a total system optimization approach. However, actual power supply systems operate by the partial optimization of individual components of the power supply system. Therefore, in this chapter, a partial optimization approach is employed to investigate the effect of electricity prices on the utilization of VRE electricity by the PTD company. The partial optimization model is used in this analysis and the objective function is the PTD company costs. The model minimizes the PTD company costs which include the cost of electricity purchase and the cost of battery storage and power transmission systems. The results show that the VRE share depends on the electricity prices. Higher prices of backup thermal power increase the utilization of VRE electricity by the PTD company. Further, the results indicate that the price difference between thermal and VRE electricity prices is a key factor in determining the utilization of VRE electricity. A price difference to obtain a target of 80 % VRE share is 54 JPY/kWh. However, considering the rate of VRE share increase, a lower price difference of 30 JPY/kWh is more

effective and obtains a 76 % VRE share. In addition, higher prices of backup thermal power increase the costs for the PTD company on the power purchase and the installation of battery storage and power transmission systems, while the revenues of power generation companies increase. To reduce the costs for the PTD company, additional measures such as carbon tax, cheaper VRE electricity prices, and subsidies to the PTD company may be effective to incentivize the costs of battery storage and the increases in the power transmission capacities.

Chapter 5 is the conclusions of the study on the effects of a combination of power fluctuation reduction measures and the study on electricity prices for power supply toward optimum VRE utilization.

Contents

Abbreviations

AMeDAS	Automated meteorological data acquisition system
CHP	Combined heat and power
EV	Electric vehicle
FIT policy	Feed-in tariff policy
GHG	Greenhouse gas
HEV	Hybrid electric vehicle
HVDC	High-voltage direct current
JPY	Japanese yen
LCOE	Levelized cost of electricity
LNG	Liquefied natural gas
LNGCC	Liquefied natural gas combined cycle
LNGOC	Liquefied natural gas open cycle
NaS battery	Sodium sulfur battery
O&M	Operation and maintenance
PSH	Pumped storage hydropower
PTD company	Power transmission and distribution company
Solar PV	Solar photovoltaic
VRE	Variable renewable energy

Nomenclature

APCost	Annual PTD company cost (JPY); Partial optimization objective function
Cha	Charging of the energy storage facility (kWh)
C-rate	Rate at which a battery is being charged or discharged
Demand	Power demand (kWh)
Dis	Discharge of the energy storage facility (kWh)
E	Power output of power plant (kWh)
ELP	Price of electricity (JPY/kWh)
ESmax	Stored energy of the storage facility (kWh)
IC	Investment cost (JPY/kW)
MC	Operation and maintenance cost (JPY/kW)
P	Power supply installed capacity (kW)
PS	Energy storage installed capacity
PT	Net power transmission (kWh)
SC	Cost of battery storage (JPY)
sd	Self-discharge rate for the energy storage facility
T	Power transmission line capacity (kW)
TC	Cost of power transmission (JPY)
TCost	Annual power supply Total cost (JPY); Total optimization objective function
TD	Total time in a year (8760 hours)
TL	Length of transmission line (km)
VC	Variable cost (JPY/kWh)

Greet letters

α	Capital cost recovery factor
η	Power loss coefficient
μc	Power supply capacity factor
μcf	Power supply capacity factor for solar and wind power
μs	Energy storage capacity factors

Superscript and subscript

1	Power (kW) component of the energy storage facility
2	Energy (kWh) component of the energy storage facility

Cha	Energy storage charging
Dis	Energy storage discharge
i	Power plant {1: Hydro, 2: Coal, 3: LNGCC, 4: LNGOC, 5: Wind, 6: Solar PV}
in, out	Power transmission into and out of a region
min, max	Minimum and maximum
r	Region {1: Central, 2: South, 3: North, 4: East}
s	Energy storage {1: Sodium-sulfur (NaS)}
t	Time (hours)
T	Transmission line
Tx	Inter-region power transmission

1 Chapter 1: Introduction

1.1 Background

Global electricity generation has increased at an annual growth rate of 2.5 % over the past decade and reached 28,466.3 TWh in 2021. Global electricity consumption is expected to continuously rise with an increase in electrification. However, more than 64 % of global electricity generation is based on fossil-fuels, a major contributor to air pollution and global climate change [1]. Climate change is currently one of the major global concerns and consented efforts are being made to mitigate greenhouse gas (GHG) emissions. The 2015 Paris Agreement set an ambitious goal of limiting global warming to well below 2°C compared to pre-industrial levels through GHG emissions reduction [2]. The reduction of GHG emissions from the power generation sector is essential for decarbonization. The development of large-scale renewable energy is an effective way to contribute to the bulk of the GHG emissions reduction in the power sector. Various renewable energy sources could play a role in decarbonizing the energy sector including hydropower, geothermal, bioenergy, and variable renewable energy (VRE) sources. Renewable energy sources will play an important role in limiting the average global surface temperature increase to below the 2 °C that is required between now and 2050 [3].

The emergence of VRE sources, which includes wind and solar photovoltaic (PV), in recent years has significantly transformed the power supply systems. The rapid decline in the costs of wind and solar PV technologies has made VRE a sustainable and economically viable alternative to conventional thermal power supply options. With supporting policy incentives, VRE deployment has grown more rapidly than other technologies and is expected to continue to increase with further technological advances. While the increased deployment of VRE is expected to increase, the integration of VRE in a power supply system poses challenges in grid operation which give rise to VRE integration costs [4]. The VRE integration costs are defined as the extra investment and operational cost of the VRE part of the power system when VRE power is integrated [5]. The VRE integration challenges have been examined in various studies [6–8]. The challenge of integrating these sources in power systems can be summarized in three key parameters; namely, scarcity, variability, and excess power supply [9]. Scarcity is when low VRE output cannot meet the relatively high demand. In such cases, other measures such as the deployment of dispatchable power sources, power imports from other systems, demand-side response, or battery storage are needed to meet power demand. Variability is the rapid fluctuation of VRE power output which requires the ramping up or down (or the start and stop) of

generation from dispatchable sources. Forecasting methodologies to accurately estimate the future wind and solar PV generation can play an important role in reducing the reaction time for the dispatchable generation sources. Excess power supply occurs during periods of low demand when large-scale VRE power is integrated into the power supply system.

Wind and solar PV are considered VRE technologies as their power output varies depending on stochastic variations in weather conditions. The power output fluctuations associated with high VRE shares necessitate measures such as geographical distribution of VRE locations, integration of battery storage, power transmission capacity enhancement, and demand-side management [10–13]. By grouping several geographically dispersed VRE power locations into a virtual unit, the intermittency of wind power can be reduced. The geographical distribution of interconnected VRE power supply reduces the effects of fluctuations in that the fluctuations of one region are offset by the output of another region. This significantly reduces the need for battery storage and backup thermal power sources required to stabilize the supply of electricity [14]. The integration of battery storage systems has been determined to facilitate the smoothening of power output from VRE power and to decrease the mismatch between power supply and demand [15,16]. Integrated battery storage systems have a significant role in realizing high VRE shares in power supply systems. Further, the enhancement of power transmission lines enables access to areas of high VRE potential. The interconnection of VRE reduces the need for battery storage and backup thermal power supply [17].

1.1.1 Geographical distribution of VRE sources

One characteristic feature of VRE sources is that they are site-specific. The power generation facilities can only be located where abundant resources are available which leads to geographical distribution. If the dispersed VRE installations are located close to the power demand, VRE power can be consumed directly by power demand, without the need for battery storage and grid enhancement. However, VRE sources not located near the demand increases integration costs as it necessitates investments in battery storage and transmission lines. One of the effective ways to reduce integration costs is to optimize the deployment of VRE over a large area with diverse weather patterns. The variation in weather patterns across greater distances has a smoothening effect that largely reduces the variability associated with the output of individual VRE sources [18,19].

Further, VRE resources are unevenly distributed over an area. This necessitates the transmission of

power from parts that have excess generation to parts with higher power demand [20]. Renewable technologies' dependence on weather also creates variability on a longer timescale. For instance, some months and years can have more wind speeds or solar radiation than others. The seasonal weather variations create month-to-month and year-to-year differences in capacity factors for VRE technologies. This can affect the estimation of the required battery storage capacity [21]. Power system resource planning and modeling can be impacted by these longer-term uncertainties and variations. Typically, power system models rely on a single weather year to estimate the potential power output of VRE sources. The choice of a weather year could lead to unintended biased estimates of the resource quality compared to a long-term average. Averages over multiple years can provide improved representations of the power systems. Furthermore, over a multi-decade period, there is potential for variability and uncertainties in VRE resources due to changes in climate conditions.

Most studies considering the interconnection of distributed VRE systems assume pre-select their locations [13,22]. However, the selection of VRE installation sites needs to be optimized based on the resource potential. Optimizing the geographical distribution reduces the effect of power output fluctuations [23]. This research optimized the geographical distribution by considering multiple candidate locations for the installation of a VRE power supply.

1.1.2 Energy storage

Energy storage facilities play a significant role in mitigating power output fluctuations of VRE and provide a basis for a renewable energy-based power supply system. Energy storage systems have a variety of applications in power systems, ranging from generation support to transmission and distribution support and consumer applications. The main role of energy storage systems is to maintain stability, facilitate the integration of renewable energy, and improve power quality. The rapid decline in energy storage costs in recent years has led to their increasing inclusion in integrated resource plans. Energy storage systems are associated with VRE sources due to their ability to synchronize power generation with power demand. Pumped storage hydropower (PSH) is the most utilized energy storage technology accounting for 99 % of energy storage installations worldwide. Other storage technologies such as batteries are increasingly being introduced [24].

The PSH system was the first generation of energy storage system constructed. A typical PSH system involves pumping water from a lower to an upper reservoir which can be scheduled on a specific

cycle of time. The PSH capacity depends on the difference in height between the upper and lower reservoirs. Presently, PSH is the largest, most sustainable, and most efficient, energy storage option that can achieve a conversion efficiency of 65–85 % [25]. Another energy storage technology is battery storage, which is basically in the category of electrochemical energy. A battery storage facility is designed to convert stored chemical energy into electrical energy. Some categories of batteries are used for high-voltage applications while others are for low-voltage. The battery system technology is the most widespread storage device for power system applications [26]. Battery systems have found application in hybrid electric vehicles (HEV), marine and sub-marine missions, aerospace operations, portable electronic systems, wireless network systems, and electrical grid network stabilization. Varieties of batteries used for different applications are available presently in the market.

The batteries are made of stacked cells in which chemical energy is converted to electrical energy and vice versa. The desired battery voltage and current capacity are obtained by connecting the cells in series and parallel. The batteries are rated in terms of their energy and power capacities. The power and energy capacities are not independent in most battery types. Currently, significant development is going on in battery technology. Different types of batteries are at various stages of commercial development while some are still in the experimental phase. The batteries used in power system applications are deep-cycle batteries (similar to the ones used in Electric vehicles) with efficiencies of about 70–80 %. The battery storage considered in this research is the sodium sulfur (NaS) batteries which are suitable for large-scale energy storage applications [27–29]. NaS batteries are a commercial energy storage technology finding applications in electric utility distribution grid support, wind power integration, and high-value service applications on islands. The round-trip ac-to-ac efficiency of NaS systems is approximately 80 %. The estimated life of a NaS battery is approximately 15 years after 4500 cycles at 90 % depth of discharge.

1.1.3 Power transmission

Transmission is an important consideration in power system models due to the regional variations in electricity demand and power supply resources. In particular, regional variations in resource availability, resource quality, and proximity of renewable resources to load can impact system-wide costs. How transmission constraints and expansion are considered can impact power system operations and have implications for the geospatial diversity in renewable energy production. There are several specific factors related to transmission and VRE that could inform the design of electricity planning

models. A greater number of model regions would enable more explicit treatments of the transmission network and renewable resources. Another factor is whether transmission and generation are co-optimized or considered separately in a planning model. Recent studies have shown the benefits of co-optimizing transmission and generation and while some actual system planners are recognizing these benefits, transmission and generation are still commonly considered separately or sequentially in many regions. As a result, ideally, models would be able to consider both approaches and communicate how different approaches would have impacts on scenario outcomes.

Technical studies have been conducted to identify grid extension as one of the measures to integrate VREs in power systems. Grid extension can smoothen fluctuations and gain access to areas of high VRE potential. The statistical advantages of interlinked VRE generation, such as the reduced need for backup and storage capacities have been quantified [17]. The power transmission in the integration of VRE power reduces the need for backup and storage facilities through the interconnection of VRE generation. Without any demand-side management and storage, transmission enhancement alone can reduce energy balancing needs by about 30 % [11]. Through grid extensions, the effects of VREs are reduced and areas of high VRE potential can be accessed. The interconnection of VRE reduces the need for energy storage and backup thermal power supply. In this research, the location of VRE sites and the capacity of transmission lines is optimized. While the effects of grid interconnections have been studied in the literature, the combined effect of the transmission enhancement and introduction of battery storage on the integration of geographically distributed VRE in power supply systems has not been investigated. This research fills that gap in the literature.

1.2 The rationale of this research

The review of previous research work and findings on power fluctuation reduction measures, clearly shows that a gap exists regarding their application. One evident gap is the lack of a comprehensive consideration of a combination of the geographical distribution of VRE locations with the introduction of battery storage and enhancement of power transmission capacity. Each of these measures has different mechanisms for reducing power fluctuations, and, therefore, the combination of these measures may be more effective than their separate application. Therefore, this research considers the combination of power fluctuation reduction measures including geographical distribution of VRE locations, power transmission enhancement, and introduction of battery storage. A total system optimization approach is used in the analysis of the effectiveness of combined measures for power

fluctuation mitigation.

Further, this research proposes and employs a combined partial and total optimization approach to increasing VRE utilization in power supply systems. Using the total optimization model approach, the optimum power supply installed capacity for a specified share of VRE in the power supply is determined. However, actual power supply systems are developed by the partial optimization of the power supply system components such as power generation, power transmission and distribution, and power demand components. In the actual power supply system, the amount of VRE electricity in the power supply from already installed power supply sources is determined by the partial optimization of a power transmission and distribution (PTD) company. Therefore, a partial optimization analysis of the PTD company is necessary to elucidate the electricity prices toward optimum social cost and variable renewable energy utilization. There is no comprehensive research that has examined the effect of wholesale electricity prices on VRE electricity utilization by the PTD company. This research bridges that gap in the literature and provides a comprehensive investigation of the pricing conditions for the PTD company to achieve the target VRE share and minimize the cost of power supply.

1.3 Objectives of the study

This research aimed to address three questions; namely, (i) What is the effective combination of technological measures for reducing the effects of VRE power output fluctuations?, (ii) What is the optimal social cost of power supply with integrated high shares of VRE?, and (iii) What are the effective electricity prices necessary to attain optimal social costs of power supply and VRE utilization?

Therefore, the objectives of this research are two-fold; (i) To determine the effective combination of technological measures to suppress the VRE fluctuations and the increase in power supply cost when high VRE shares are integrated, and (ii) To elucidate the effective conditions of electricity prices required to achieve optimum VRE utilization.

1.4 Structure of thesis

This dissertation consists of 5 chapters, and the summary of each chapter is as follows: Chapter 1 summarizes the literature review and provides the objectives of the research. Chapter 2 presents a description of the analysis methods and the case study area. The analysis methodology involves the development of two linear programming-based total and partial optimization models namely; total

optimization and partial optimization. The total optimization model is used to examine the effects of power fluctuation mitigation measures on the integration of large-scale VRE in power supply systems. The partial optimization model is used in the analysis of electricity price effects on the utilization of VRE electricity by the power transmission and distribution (PTD) component of the power supply system. Chapter 3 is a study on effective measures for power fluctuation mitigation of geographically distributed wind and solar power. This analysis considers power fluctuation mitigation measures, including the introduction of battery storage and enhancement of power transmission capacity. The study employs a total optimization approach to determine the effective combination of fluctuation reduction measures toward the minimized total cost of power supply. Chapter 4 is a study on electricity prices for power supply toward an optimum VRE utilization. In chapter 3, a model of the entire power supply system is determined through a total system optimization approach. However, the actual power supply systems operate by the partial optimization of individual components of the power supply system. Therefore, in chapter 4, a partial optimization approach is employed to investigate the effect of electricity prices on the utilization of VRE electricity. This analysis determines the effective pricing conditions for increasing the purchase of VRE electricity by the PTD company. Finally, Chapter 5 summarizes the conclusions of the study on the effective combination of power fluctuation reduction measures and the study on effective electricity prices for power supply toward optimum VRE utilization.

2 Chapter 2: Methodology

2.1 Model description

Nomenclature of optimized variables

$APCost$	Annual cost for the PTD company (JPY); Partial optimization objective function
$TCost$	Total annual cost of the power supply (JPY); Total optimization objective function
$E_{i,t,r}$	Power output of power plant i at time t (kWh) in region r
$P_{i,r}$	Installed capacity of power plant i in region r (kW)
$Cha_{s,t,r}$	Charging of the energy storage facility s at time t in region r (kWh)
$Dis_{s,t,r}$	Discharge of the energy storage facility s at time t in region r (kWh)
$ESmax_{s,t,r}$	Stored energy of the storage facility s at time t in region r (kWh)
$PS^1_{s,r}$	kW capacity of the energy storage facility s in region r (kW)
$PS^2_{s,r}$	kWh capacity of the energy storage facility s in region r (kWh)
T_r	Power Transmission line capacity from the central region to region r (kW)
$T^{in}_{t,r}$	Power transmitted into the central region at time t from region r (kWh)
$T^{out}_{t,r}$	Power transmitted from the central region at time t to region r (kWh);
Where,	
r (region) $\in$	{1: Central, 2: South, 3: North, 4: East}
i (power supply) $\in$	{1: Hydro*, 2: Coal*, 3: LNGCC 4: Wind*, 5: Solar PV*},
s (energy storage) $\in$	{1: NaS battery}
r (For transmission) $\in$	{1: $T_1 = T^{in}_{t,1} = T^{out}_{t,1} = 0$, 2: Central-South, 3: Central-North, 4: Central-East}
*****exogenous in the partial system optimization	

Power system modeling provides the tools for assessing the effective integration of high VRE shares. Power supply system modeling is the systematic forecasting of the power supply and power demand based on changes in specific conditions. It has been established in the literature that to be feasible, power supply system modeling must ensure that it meets four primary requirements. First, the electricity supply must be matched to a realistically projected electricity demand. Second, the proposed electricity supply must be capable of meeting the real-time electricity demand. Third, any transmission requirements for newly installed capacity must be considered to demonstrate the delivery of generated electricity to the projected electricity demand. Fourth, the proposed system must show how critical

supporting technologies such as energy storage will be provided to ensure power quality and the reliable operation of the power supply system. The models developed in this research meet the above criteria by (i) considering actual power demand data from the case study area, (ii) ensuring that power supply meets the power demand on an hourly basis, (iii) providing for power transmission enhancement, (iv) providing for the introduction of energy storage systems.

2.1.1 A total system optimization model

A linear programming-based power supply optimization model is developed with an objective function of minimizing the total annual cost of power supply while meeting the power generation conditions that are provided by constraint equations. The annual cost includes the annualized investment costs, operation and maintenance costs, and variable costs of the power supply facilities, power transmission lines, and battery storage facilities. The solution of the optimization model is a minimized total annual cost of power supply *(TCost)* which is defined in Eq. (2.1.1).

$$min.TCost = \sum_{r=1}^{4}\left\{\sum_{i=1}^{6}\left((\alpha_i\, IC_i + MC_i)\; P_{i,r} + \sum_{t=1}^{TD} VC_i\, E_{i,t,r}\right) + TC_r + SC_{s,r}\right\} \qquad (2.1.1)$$

Where α_i is the annual capital cost recovery factor of power plant i; IC_i is the investment cost (JPY/kW) of power plant i; MC_i is the operation and maintenance cost (JPY/kW) of power plant i; VC_i is the variable cost (JPY/kWh) of power plant i; t is the time (hours), and TD is the total time in a year (8760 hours). The power plant lifespan is accounted for in the capital cost recovery factor α_i. The cost of power transmission TC_r is defined in Eq. (2.1.2).

$$TC_r = (\alpha_T\, IC_T TL_r + MC_T)\; T_r + \sum_{t=1}^{TD} VC_T\left(T_{t,r}^{in} + T_{t,r}^{out}\right) \qquad (2.1.2)$$

Where: α_T is the capital cost recovery factor, IC_T is the investment costs of power transmission capacity (JPY/kW/km), MC_T is the operation and maintenance cost (JPY/kW), and VC_T is the variable cost for power transmission (JPY/kWh), and TL_r is the length of transmission line r. The battery storage used in this model is the sodium sulfur (NaS) battery which has a power (kW) and an energy (kWh) component of its capacity. The cost of battery storage $SC_{s,r,}$ is defined in Eq. (2.1.3);

$$SC_{s,r} = \sum_{s=1}^{1}\left(\left(\alpha_s^1\, IC_s^1\, PS_{s,r}^1\right) + \left(\alpha_s^2\, IC_s^2\, PS_{s,r}^2\right) + \sum_{t=1}^{TD} VS_s\, Cha_{s,r,t}\right) \quad (2.1.3)$$

Where: α^1_s is the annual fixed cost recovery factor for the power component of storage facility *s*, α^2_s is the annual fixed cost recovery factor for the energy component of storage facility *s*, IC^1_s is the fixed cost of the power component of storage facility *s* (JPY/kW), IC^2_s is the fixed cost of the energy component of storage facility *s* (JPY/kWh), and VS_s is the variable cost for materials such as electrodes and electrolytes (JPY/kWh).

The generic power supply and demand balance is illustrated by Eq. (2.1.4). The balance between the power supply and demand is constrained such that the sum of the output of power supply facilities, the net discharge of battery storage facilities, and the net power transmission should be able to meet the power demand at each region *r*, and each time, *t.*

$$\sum_{i=1}^{6} E_{i,t,r} + \sum_{s=1}^{1}\left(\eta_{Dis}\, Dis_{s,t,r} - Cha_{s,t,r}/\eta_{Cha}\right) + PT_{t,r} \geq Demand_{t,r} \quad (2.1.4)$$

Where η represents the power loss coefficient which accounts for losses during power discharge η_{Dis}, charging η_{Cha}, and inter-region power transmission η_{Tx}, and $Demand_{t,r}$ is the power demand at time *t* in region *r* (kWh). With the power discharge and charging, losses inbuilt into the model, the simultaneous charging and discharging of the battery storage system does not occur at each given time *t*. Only charging or discharging occurs at each given time *t*. Eq. (2.1.4) is an inequality equation that enables the estimation of excess power generation due to the fluctuations in the VRE output. Power interchange among the four regions is facilitated by the interconnection through the central region. The third term on the right-hand side of Eq. (2.1.4) represents the net power transmission $PT_{t,r}$ in each region and is illustrated in Eq. (2.1.5) for the central (*r*=1), south (*r*=2), north (*r*=3), and east (*r*=4) regions.

$$\begin{aligned}
PT_{t,r=1} &= \eta_{Tx}\left(T_{t,2}^{in} + T_{t,3}^{in} + T_{t,4}^{in}\right) - \left(T_{t,2}^{out} + T_{t,3}^{out} + T_{t,4}^{out}\right);\\
PT_{t,r=2} &= \eta_{Tx}\, T_{t,2}^{out} - T_{t,2}^{in};\\
PT_{t,r=3} &= \eta_{Tx}\, T_{t,3}^{out} - T_{t,3}^{in};\\
PT_{t,r=4} &= \eta_{Tx}\, T_{t,4}^{out} - T_{t,4}^{in}
\end{aligned} \quad (2.1.5)$$

Equations (2.1.6) ~ (2.1.9) are the minimum and maximum capacity constraints for the power plants, battery storage, and power transmission facilities. These constraints eliminate negative power generation in the optimization solution. Equations (2.1.10) ~ (2.1.14) account for capacity factors for power plants and storage facilities. Where: $P^{min}_{i,r}$, $PS^{1min}_{s,r}$, $PS^{2min}_{s,r}$, T^{min}_{r} are minimum capacities, $P^{max}_{i,r}$, $PS^{1max}_{s,r}$, $PS^{2max}_{s,r}$, T^{max}_{r} are maximum capacities, $\mu c_{i,r,t}$ is the capacity factor for hydro and coal power; $\mu c^{min}_{i,r}$ and $\mu c^{max}_{i,r}$ are the minimum and maximum capacity factors for LNGCC and LNGOC; $\mu cf_{i,r,t}$ is the VRE capacity factor of wind and solar PV; $\mu s^{1min}_{s,r}$ and $\mu s^{1max}_{s,r}$ are the minimum and maximum capacity factors, and $\mu s^{2min}_{s,r}$ and $\mu s^{2max}_{s,r}$ are the minimum and maximum states of charge for storage facility s.

$$P^{min}_{i,r} \le P_{i,r} \le P^{max}_{i,r} \quad (2.1.6)$$

$$PS^{1min}_{s,r} \le PS^{1}_{s,r} \le PS^{1max}_{s,r} \quad (2.1.7)$$

$$PS^{2min}_{s,r} \le PS^{2}_{s,r} \le PS^{2max}_{s,r} \quad (2.1.8)$$

$$T^{min}_{r} \le T_{r} \le T^{max}_{r} \quad (2.1.9)$$

$$E_{i,r,t} = \mu c_{i,r,t} P_{i,r} \quad (i = 1,2) \quad (2.1.10)$$

$$\mu c^{min}_{i,r} P_{i,r} \le E_{i,r,t} \le \mu c^{max}_{i,r} P_{i,r} \quad (i = 3,4) \quad (2.1.11)$$

$$E_{i,r,t} = \mu cf_{i,r,t} P_{i,r} \quad (i = 5,6) \quad (2.1.12)$$

$$\mu s^{1min}_{s,r} PS^{1}_{s,r} \le Cha_{s,r,t} + Dis_{s,r,t} \le \mu s^{1max}_{s,r} PS^{1}_{s,r} \quad (2.1.13)$$

$$\mu s^{2min}_{s,r} PS^{2}_{s,r} \le ESmax_{s,r,t} \le \mu s^{2max}_{s,r} PS^{2}_{s,r} \quad (2.1.14)$$

The operation of the battery storage facilities considered in this model is constrained as in Eq. (2.1.15) which expresses the balance between the net energy discharge and the amount of energy available in the battery storage facilities at time t. Where sd_s is the self-discharge rate.

$$ESmax_{s,r,t} = (1 - sd_s)\, ESmax_{s,r,t-1} + \left(Cha_{s,i,t} - Dis_{s,r,t}\right) \quad (2.1.15)$$

The power capacity and energy capacity of the storage facilities are related by the power conversion ratio, the *C-rate*, which is a measure of the rate at which a battery is being charged or discharged, as expressed in Eq. (2.1.16).

$$PS^{1}_{s,r} \le C\text{-}rate_s\, PS^{2}_{s,r} \quad (2.1.16)$$

In this study, the VRE share is an input parameter defined as the ratio of power supply from wind and solar PV power to the total power demand and is constrained by Eq. (2.1.17).

$$(1 - VRE_{share}) \sum_{r=1}^{4} \sum_{t=1}^{TD} Demand_{t,r} = \sum_{r=1}^{4} \sum_{t=1}^{TD} \sum_{i=1}^{4} E_{i,t,r} \qquad (i = 1, 2, 3, 4) \tag{2.1.17}$$

2.1.2 A partial system optimization model

A linear programming-based partial optimization model is developed and used for partial optimization analysis. The objective function is to minimize the cost for the PTD company, while the objective function in section 2.1.1 is to minimize the total cost of power supply. In this study, it is assumed that the PTD company covers the cost of the installation and operation of the power transmission and storage facilities. Therefore, the PTD company cost includes the cost of purchasing electricity from power suppliers and the cost of installing and operating battery storage and transmission facilities. The solution of the objective function (*APCost*) is defined in Eq. (2.1.18).

$$min.\, APCost = \sum_{r=1}^{4} \left\{ \left(\sum_{i=1}^{4} \sum_{t=1}^{TD} ElP_i \, E_{i,t,r} \right) + SC_{s,r} + TC_r \right\} \tag{2.1.18}$$

Where ELP_i is the price of electricity (JPY/kWh) from the power generating source i; t is the time (hours), and TD is the total time in a year (8760 hours). The costs of setting up and maintaining the power transmission TC_r and battery storage $SC_{s,r}$ facilities are defined in Eq. (2.1.19) and Eq. (2.1.20), respectively.

$$SC_{s,r} = \sum_{s=1}^{1} \left(\left(\alpha_s^1 \, IC_s^1 \, PS_{s,r}^1 \right) + \left(\alpha_s^2 \, IC_s^2 \, PS_{s,r}^2 \right) + \sum_{t=1}^{TD} VS_s \, Cha_{s,r,t} \right) \tag{2.1.19}$$

$$TC_r = \left(\alpha_T \, IC_T TL_r + MC_T \right) T_r + \sum_{t=1}^{TD} VC_T \left(T_{t,r}^{in} + T_{t,r}^{out} \right) \tag{2.1.20}$$

Where in Eq. (2.1.19): $\alpha^1{}_s$ is the annual fixed cost recovery factor for the power component of storage facility s, $\alpha^2{}_s$ is the annual fixed cost recovery factor for the energy component of storage facility s, $IC^1{}_s$ is the fixed cost of the power component of storage facility s (JPY/kW), $IC^2{}_s$ is the fixed cost of the energy component of storage facility s (JPY/kWh), and VS_s is the variable cost for materials such

as electrodes and electrolytes (JPY/kWh). In Eq. (2.1.20): α_T is the capital cost recovery factor, IC_T is the investment costs of power transmission capacity (JPY/kW/km), MC_T is the operation and maintenance cost (JPY/kW), and VC_T is the variable cost for power transmission (JPY/kWh), and TL_r is the length of transmission line r. The battery storage used in this model is the sodium sulfur (NaS) battery which has a power (kW) and an energy (kWh) component of its capacity.

In addition to the above equations, the model has constraint equations on the energy balance, power supply, storage, and transmission installed capacity constraints, and constraints on power supply capacity factors. The detailed description of the rest of the optimization model is the same as the model presented in section 2.1.1.

2.2 Fluctuations in renewable energy output

2.2.1 Fluctuations in wind power output

This section describes the method used to calculate wind power output variability in this study. The hourly capacity factor profiles of solar and wind power were estimated based on the AMeDAS meteorological data for 193 observation points in Hokkaido in 2014. The observation points with the highest capacity factors were selected for each area and used as the "representative" hourly capacity factor profiles of that area. There are several manufacturers of wind turbines with differences in wind turbine performance. This research considered a 1000 kW class of wind turbines (MWT-1000) manufactured by Mitsubishi Heavy Industries, Ltd for the estimation of wind power capacity factors. The wind turbine is designed not to generate power at wind speeds below 3.0 m/s, and at higher wind speeds, its output increases as the wind speed increases, but when the wind speed reaches 13.5 m/s, it operates stably at its rated output of 1000 kW. However, when the wind speed exceeds 25 m/s, the operation is forcibly stopped for safety reasons. The turbines have cut-in and cut-out wind speeds of 3 m/s and 25 m/s respectively, a hub height of 69 m, and a rotor diameter of 61.4 m. The wind speed data observed by an anemometer at an AMeDAS station was converted to wind speed data at the hub height of the wind turbine using the power law, Equation (2.2.1).

$$U(z) = U_0(z_0) \times (z/z_0)^{1/w} \tag{2.2.1}$$

where z is the height above ground of the wind turbine hub, z_0 is the height above ground of the

anemometer installed at the AMeDAS stations in each region (reference altitude), U(z): wind speed at ground level Z, U(z0): wind speed at reference altitude, 1/w: power index (roughness of ground surface condition). The power law index is a coefficient that expresses the state of roughness of the ground surface and was set to 0.2, which is more applicable over open land surfaces. The obtained altitude correction factor $(z/z_0)^{(1/w)}$ for each region was multiplied by the wind speed at each hour to convert it to the wind speed at the height of the windmill hub, and the hourly wind power output was obtained.

2.2.2 Fluctuations in solar PV output

The following is a description of the method used to calculate PV power output variability in this study. The method and parameters are based on the Solar Energy Utilization Handbook and the JIS standard methods for estimating the amount of electricity generated by photovoltaic power generation systems. Solar panels used for photovoltaic power generation are installed at an angle to the ground surface, so it is necessary to determine the amount of solar radiation incident on such a slope or slope irradiance. The slope irradiance $I_{\beta\gamma}$ is decomposed into the direct component $I_{b\beta\gamma}$, the ground reflection component $I_{r\beta\gamma}$, and the sky scattering component $I_{s\beta\gamma}$, and is expressed by the following equation.

$$I_{\beta\gamma} = I_{b\beta\gamma} + I_{r\beta\gamma} + I_{s\beta\gamma} \tag{2.2.2}$$

In Fig. 2.1 (a), the zenith angle of the sun is θ_z and the slope angle is β. If the solar radiation perpendicular to the sun is denoted as I_n, the direct component I_b received by the horizontal surface and the direct component $I_{b\beta\gamma}$ received by the slope and the ratio of the two, r_b, are expressed by the following equations.

$$Ib = In\cos\theta z \tag{2.2.3}$$

$$Ib\beta\gamma = In\cos\theta \tag{2.2.4}$$

$$rb = Ib\beta\gamma / Ib = \cos\theta / \cos\theta z \tag{2.2.5}$$

Where $cos\theta$ and $cos\theta_z$ are the points N, S, and h in Figure 2.1 (b) where the perpendicular line to the slope intersects the celestial sphere. The solar declination is derived from the latitude of the observation point and the solar equatorial latitude.

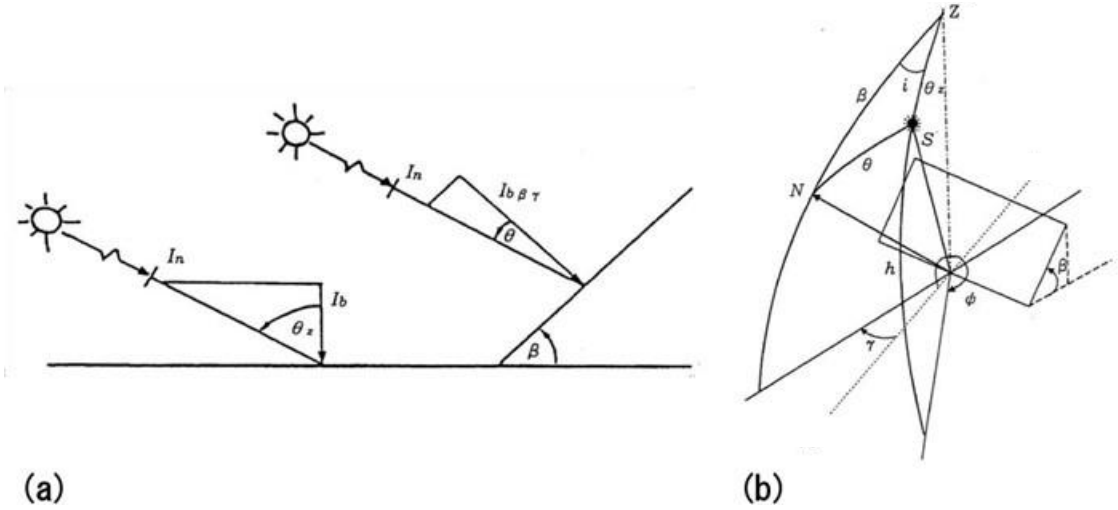

Fig. 2.1. Incidence angle of sunlight

The ground reflection component $I_{r\beta\gamma}$ is estimated by the uniform reflection model and is expressed by the following equation.

$$I_{r\beta\gamma} = I_\rho(1 - \cos\beta)/2 \tag{2.2.6}$$

In this model, it is assumed that the solar radiation reaching the ground surface is reflected with the same intensity in all directions at the ground surface. The reflectivity ρ of the ground surface is calculated from Japanese meteorological agency data. The sky scattering component $I_{s\beta\gamma}$ is estimated by Hay's model and is expressed by the following equation.

$$I_{s\beta\gamma} = I_d[\{I - I_d/I_0\}\cos\theta/\cos\theta_z + \{(1 - (I - I_d)/I_0\}(1 - \cos\beta)/2] \tag{2.2.7}$$

In this model, the sky-scattered solar radiation, (I (-Id)/I_0 is treated as the direct component of solar ambient light, and the remainder is assumed to be uniformly distributed in the sky. The scattering component of solar radiation, I_d, is calculated from the clear-sky index and the *Erbs* equation, where I is the hourly integrated solar radiation and I_0 is the horizontal solar radiation outside the atmosphere. The relationship between the slope irradiance $I_{\beta\gamma}$ calculated by these equations and the amount of electricity generated per unit time by the solar panels per unit installed capacity pt is shown in the following equation.

$$p_t = I_{\beta\gamma} \times K_{PT} \times K_P \times K_H \times K_C \quad (2.2.8)$$

Each correction factor in this formula is derived. K_{PT} is the correction factor due to dirt on the panel surface, array circuits, etc., K_H is the correction factor due to solar radiation, etc., and K_C is the correction factor at the power conditioner. In this study, the amount of electricity generated by photovoltaic power generation is only determined by the aforementioned slope irradiance and correction factors.

2.3 Case study area

Hokkaido, the northernmost prefecture of Japan, is selected as a case study area due to its large capacity for wind power. Since the introduction of the Feed-in Tariff (FIT) policy in 2012, renewable energy generation in Japan has increased significantly from 9 % in 2011 to 15 % in 2016, making renewable energy the third largest energy source after liquefied natural gas (LNG) and coal [30]. Solar PV, in particular, has played a significant role in the increase in renewable electricity generation, while the increase in wind power, which has a high potential capacity factor in Hokkaido, has not been significant [31]. For analysis purposes, the area was divided into four geographical regions: north, east, south, and central Hokkaido. Figure 2.1 (a) shows a model of the power demand distribution and power transmission. As this study's focus is on energy balance within Hokkaido, the existing 900 MW high-voltage, direct current (HVDC) interconnection with Honshu is not considered in the analysis. The names of the numbered locations and their respective average annual capacity factors are listed in Tables 2.1 and 2.2. The restrictions on land use and area due to the introduction of wind and solar power were not considered in this analysis. Solar PV potential is concentrated in the eastern and central regions of Hokkaido. The other regions have relatively lower annual capacity factors for solar PV generation. Figure 2.1 (b) shows the geographical locations of 20 wind power and 10 solar PV power candidate sites which were pre-selected based on having the highest power generation capacity factors as estimated from the AMeDAS meteorological data for observation sites throughout Hokkaido. With this figure, the potentially uneven distribution of wind and solar power generation locations and the power transmission capacity between regions can be visualized. The solar PV potential is concentrated in the eastern and central regions, with Hidakamonbetsu (site 1) and Sarabetsu (site 4) having the highest average annual solar PV capacity factors of 12.7 %. For wind power, Koetoi (site 9) has the highest average annual capacity factor of 39.7 %.

Table 2.1. Capacity factors of selected wind power locations.

Region	Location		Capacity Factor [%]
Central	[1]	Hamamasu	23.0
	[2]	Chitose	19.6
	[3]	Muroran	19.1
	[4]	Urakawa	16.5
	[5]	Suttsu	14.9
South	[6]	Esashi	25.2
	[7]	Setana	23.4
	[8]	Takamatsu	17.5
North	[9]	Koetoi	39.7
	[10]	Rumoi	26.6
	[11]	Hamaonishibetsu	26.6
	[12]	Mashike	22.5
	[13]	Teshio	21.0
	[14]	Hatsuyamabetsu	20.6
	[15]	Wakkanai	18.4
East	[16]	Nosappu	24.8
	[17]	Nemuro	22.0
	[18]	Teshikaga	17.5
	[19]	Tokoro	16.3
	[20]	Kushiro	15.4

Table 2.2. Capacity factors of selected solar PV locations.

Region	Spot		Capacity Factor [%]
Central	[1]	Hidakamonbetsu	12.7
	[2]	Mukawa	12.6
	[3]	Shizunai	12.5
East	[4]	Kamisatsunai	12.6
	[5]	Sarabetsu	12.7
	[6]	Taiki	12.6
	[7]	Nukanai	12.5
	[8]	Otsu	12.4
	[9]	Urahoro	12.4
	[10]	Ikeda	12.4

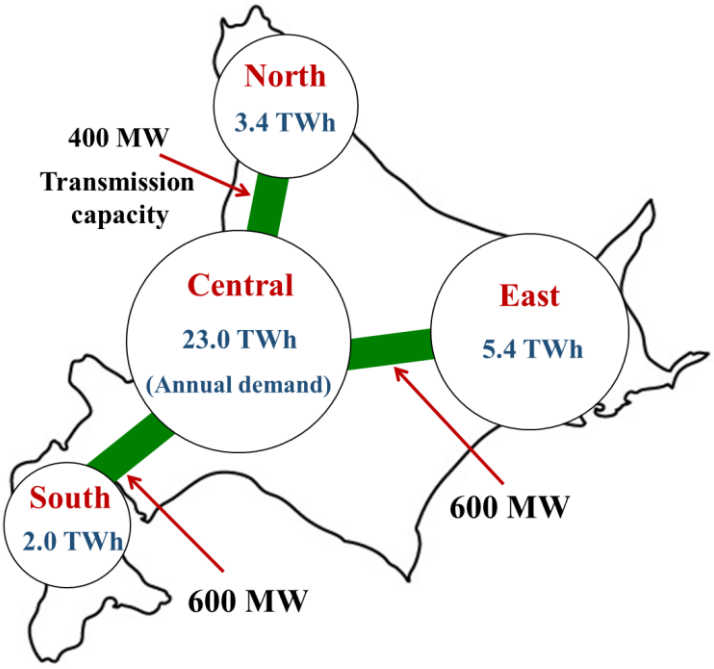

(a) Distribution of annual power demand and power transmission capacity.

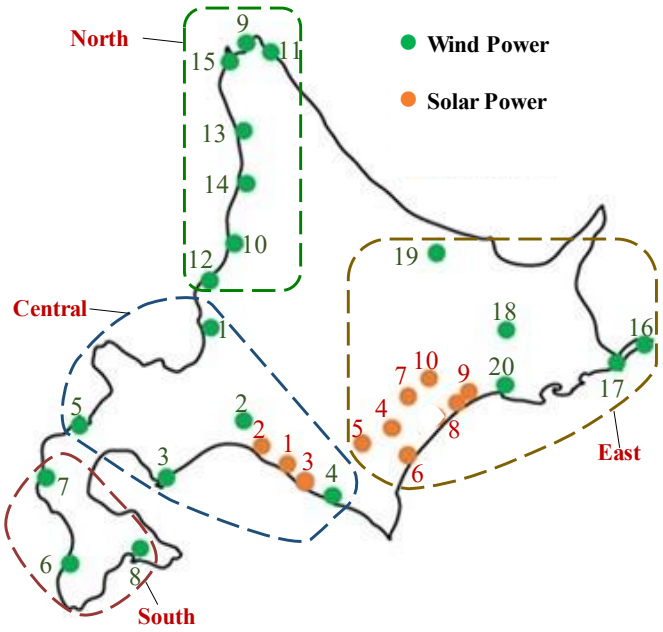

(b) Geographical distribution of 20 wind power and 10 solar PV power candidate locations.

Fig. 2.2. Study area power supply system. (a) Distribution of annual power demand and power transmission capacity. (b) Geographical distribution of 20 wind power and 10 solar PV power candidate locations.

The hourly capacity factor profiles of solar and wind power were estimated based on the AMeDAS meteorological data for 193 observation points in Hokkaido in 2014 [32]. The observation points with the highest capacity factors were selected for each area and used as the "representative" hourly capacity factor profiles of that area. For solar power, solar irradiation, air temperature, and snow coverage data were converted to the output rates using geographic characteristics (latitude and longitude) and assumptions of solar panel characteristics (tilt angle, system output coefficients of panels) [33]. The capacity factor curves for wind power plants assumed in this study were based on a standard 2 MW wind turbine with a 70 m hub height and cut-in, rated, and cut-out wind speeds were set to 3, 12, and 25 m/s, respectively [23,34]. Figure 2.2 shows the annual capacity factor profiles of solar PV site 1 and wind site 9 in hourly intervals. The capacity factor of solar power is high during the daytime, and the seasonal trend is such that it is high in spring and low in summer. The wind power capacity factor displays irregular daily fluctuations and is generally consistent throughout the year but is slightly higher in winter and lower in summer.

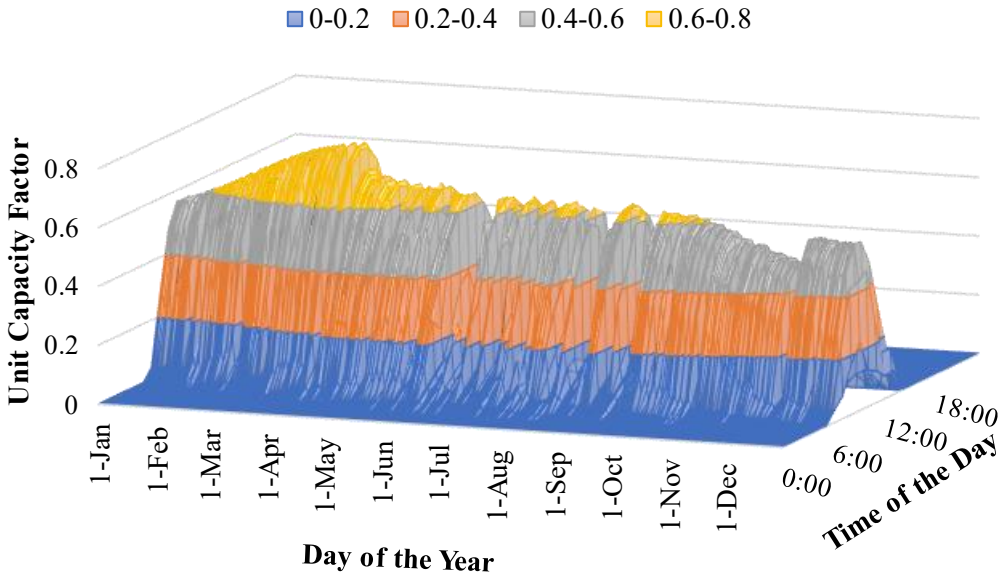

(a) Solar PV capacity factor for Hidakamonbetsu (site 1)

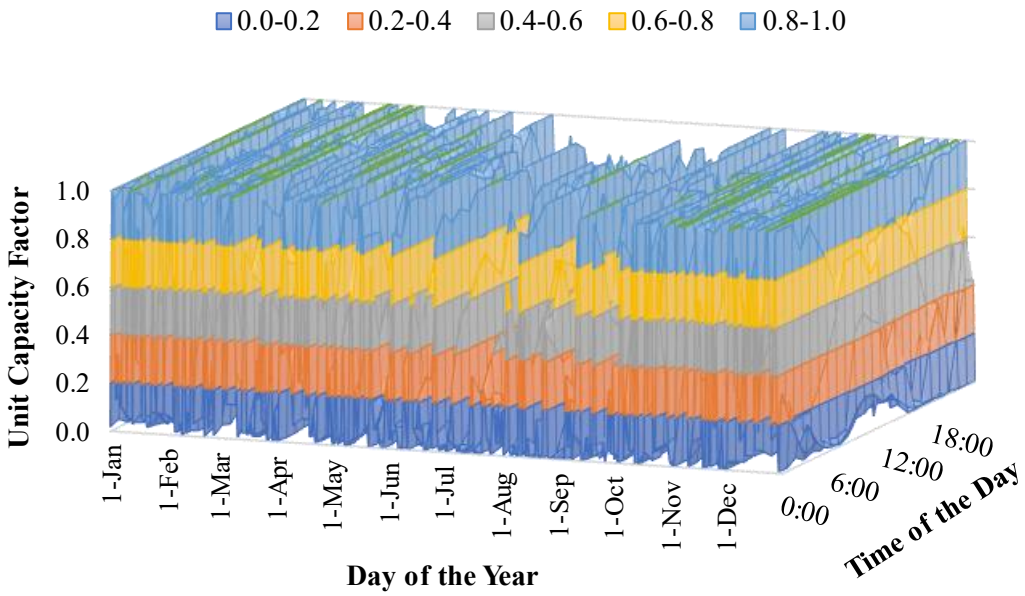

(b) wind power capacity factor for Koetoi (site 9)

Fig. 2.3. Variation of the capacity factor for a 1-year duration on an hourly interval. (a) Solar PV capacity factor, and (b) wind power capacity factor.

2.3.1 Electricity supply

The power supply in Hokkaido was modeled to be comprised of coal thermal power and hydropower as baseload power sources with a constant output, solar PV, and wind power as the VRE sources, while liquefied natural gas open cycle (LNGOC) and liquefied natural gas combined cycle (LNGCC) thermal power are the backup power sources available for load management. Currently (FY2020), the power supply in Hokkaido comprises renewable energy electricity at 19 % (including hydro, biomass, geothermal, and VRE power) of which VRE power purchased under the FIT policy is at 8 % of the total power supply. The thermal power supply includes coal-fired thermal power at 38 %, LNG thermal power at 11 %, and oil-thermal power at 8 % of the total power supply [35].

In this study, LNGCC and coal thermal power were assumed to be installed only in the central region. The installed capacities of coal, LNGCC, LNGOC, solar PV, and wind power infrastructure to be installed were determined from the optimization model. Even though hydropower is a dispatchable

power source, in this analysis it was assumed as a baseload with constant output as it accounted for only about 10 % of the power demand and no additional large-scale hydropower would be installed.

Regarding battery storage, while pumped storage hydropower (PSH) remains the most utilized battery storage technology accounting for 99 % of battery storage installations worldwide, other battery storage technologies such as batteries are increasingly being introduced [24]. However, since PSH storage is considered to be at or close to its practical limit in Japan [36] and it is uncertain if the existing 600 MW PSH in Hokkaido will still be operational in 2050, this research did not include PSH. This research considered the introduction of large-capacity sodium sulfur (NaS) batteries, rechargeable oxidation-reduction batteries suitable for large-scale battery storage applications. NaS batteries are one of the advanced battery storage technologies for high-energy applications, with a cycle efficiency of 85 %, a self-discharge rate of 0.10 %, and an hourly charge-discharge rate (C-rate) of 0.17 [27–29]. If PSH was considered, the capacity of NaS batteries to be introduced would be less than the capacity obtained in this analysis.

2.3.2 Electricity demand

This analysis in this research focuses on integrating an increasing share of solar PV and wind in the power supply mix while minimizing the total cost of the power supply in Hokkaido in 2050. The hourly time-resolved (8760 hours from 1st January to 31st December 2014) power demand data used in this analysis is based on the power demand data for 2014 obtained from Hokkaido Power Electric company's past power usage database [37]. The 2014 total power demand data, which was reported as 33.8 TWh, is not significantly different from the current (2020) total power demand of 30.4 TWh [38]. According to government projections [39], electricity generation in Japan will remain stable over the period to 2030, as the lower demand from a declining population and energy efficiency improvements outweigh the increasing electricity demand from economic growth and electrification of the economy. Therefore, this study assumes that the total power demand in Hokkaido in 2050 will be similar to that in 2014 [40].

The power demand distribution in the northern, eastern, southern, and central sub-regions as shown in Fig. 2.3 was estimated based on the population distribution in the four regions [41]. The central region with 68 % of the population of Hokkaido requires an estimated power demand of 23.0 TWh, the eastern region with 16 % of the population requires 5.4 TWh, the northern region with 10 % becomes 3.4 TWh, and the southern region with 6 % needs 2.0 TWh. Figure 3 shows the monthly

power demand in Hokkaido, characterized by a decrease in demand in summer and increased demand in winter. The increase in power demand is due to the increase in heating and lighting due to the extreme winter and fewer daylight hours. The electricity demand tends to be low in the evening in the spring and low in the summer.

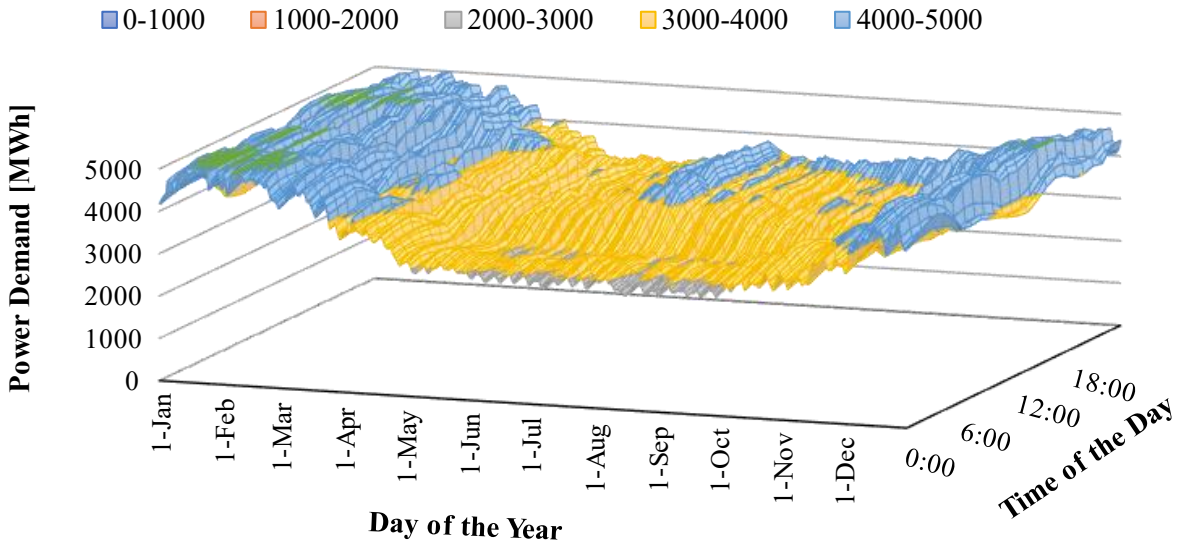

Fig. 2.4. Variation of power demand for a 1-year duration on an hourly interval for all of Hokkaido.

2.3.3 Assumptions, cost, and technical input parameters

The power supply, transmission, and storage costs that are used for 2050 are based on the 2030 cost projections by the Agency for Natural Resources and Energy of Japan [42]. Table 2.1 shows the costs and technical input parameters for power plants and Table 2.2 shows the cost and technical parameters for power transmission and battery storage facilities. Other assumptions in this research include ; (i) no distinction is made between existing and new power generation facilities, and initial and running costs are calculated for both, (ii) excess VRE electricity which is not used in battery charging and is not transmitted to other regions is assumed to be discarded and is simply calculated as a reduction in facility utilization, (iii) the analysis does not consider the cost of reinforcing transmission and distribution lines within the same area due to the installation of power generation facilities, and (iv) Only LNGCC and LNGOC are assumed as backup power sources whose output can be adjusted to meet fluctuations in electricity demand and VRE output.

Table 2.3. Cost and technical parameters for the power supply sources.

		Hydro	Coal	LNGCC	LNGOC	Wind	Solar
Initial cost	[10^3 JPY/kW]	640	250	120	83.8	252	222
Fixed O&M	[10^3 JPY/kW/year]	9.1	10	3.7	0.74	5.3	3.2
Variable cost	[JPY/kWh]	0.2	9.1	14	16	0.3	0.2
Useful life	[year]	40	40	40	40	20	30
Capacity factor		0.40	0.70	-	-	Site-specific	Site-specific
Min. capacity	[MW]	965	0	1708	0	0	0
Max. capacity	[MW]	965	-	-	-	-	-

Table 2.4. Cost and technical parameters for battery storage and power transmission facilities.

Cost items		Transmission
Initial cost	[10^3 JPY/kW/km]	1315
Fixed O&M	[10^3 JPY/kW/year]	9.9
Variable O&M	[JPY/kWh]	0
Useful life	[year]	50
Transmission efficiency		0.97
Minimum capacity	[MW]	600, 400, 600
Cost items		NaS battery
Initial cost	[10^3 JPY/kW]	47.4
Initial cost	[10^3 JPY/kWh]	38.6
Fixed O&M	[10^3 JPY/kW/year]	3.4
Variable O&M	[JPY/kWh]	0.23
Useful life	[year]	15
Self-discharge loss	[1/hour]	0.001
Cycle efficiency		0.85
Charge and discharge efficiency		0.92
C-rate	[1/hour]	0.17

3 Chapter 3: Analysis of effective measures for power fluctuation mitigation of geographically distributed wind and solar power

3.1 Introduction

In 2019, global electricity generation grew by 1.35 % and the share of renewables in power generation increased from 9.3 % to 10.4 %, compared to 2018. However, fossil-fueled power generation, a major contributor to greenhouse gas (GHG) emissions, still constitutes more than 64 % of the world's electricity generation [43] and accounts for more than two-thirds of global GHG emissions [44]. Reducing GHG emissions in the power sector will play a fundamental role in the global move towards decarbonization. The development of large-scale renewable energy is an effective way to contribute to the bulk of the greenhouse gas emissions reduction in the power sector that is required between now and 2050 for limiting the average global surface temperature below 2 °C [3]. According to the [45], to achieve the below 2 °C scenarios, the contribution of renewable energy to the global electricity supply must increase to 25 % by 2040. In recent years, there has been a rapid increase in the development of variable renewable energy (VRE), which includes solar photovoltaic (PV) and wind power, largely driven by the decreasing generation costs and financial support from governments.

While the increased deployment of renewable energy offers promising benefits such as reduced GHG emissions and increased energy security, there are challenges associated with VRE due to the intermittency, non-dispatchable feature, and uncertain energy output. Ueckerdt et al. (2015) have demonstrated that the effects of power output fluctuations increase with the increase in the share of solar and wind power [46]. Therefore, the development of power systems should aim at minimizing the effects of VRE power fluctuations. Among the VRE power fluctuation reduction measures, the geographical distribution of VRE locations, integration of battery storage, and enhancement of power transmission lines play a significant role in mitigating the effects of fluctuations of VRE power output and are the focus of this study. The individual effects of these measures on the power systems are increasingly being explored by researchers. Obara et al. (2015) and Ziger et. al. (2015) examined the effects of the geographical distribution of interconnected VRE locations over a large area and concluded that the effective distribution of VRE locations reduces the effects of fluctuations in the fluctuations of one facility may be offset by the output of another facility [13,14]. The appropriate distribution of VRE facilities was also determined to significantly reduce the cost of backup thermal power sources required to stabilize the supply of electricity and the need for transmission grid

reinforcements [20,47].

The integration of battery storage systems has been determined to facilitate the smoothening of power output from VRE power and to decrease the mismatch between power demand and supply [15]. Other studies established that battery storage has a significant role in realizing a 100 % renewable energy-based power system [36,48–50]. In addition, some studies have examined the effects of power transmission grid enhancement in reducing fluctuations and gaining access to areas of high VRE potential. Heide et al. (2010) and Becker et al. (2014) investigated the role of power transmission in the integration of VRE power and determined that the interconnection of VRE generation reduces the need for backup and storage facilities [17]. Becker et al. (2014) further estimated that without any demand-side management and storage, transmission enhancement alone can reduce energy balancing needs by about 30 % [11]. Schaber et al. (2012) concluded that through grid extensions, the effects of VREs are reduced and benefits can be created mainly in baseload technologies, through more homogeneous and stable electricity prices and larger revenues [51].

While the above literature demonstrates the significance of each of the VRE power fluctuation mitigation measures, no study has considered the effects of a combination of these three measures. These measures have different mechanisms to reduce the wastage of power, and the combination of these measures may be more effective than their separate usage. Such a combined effect study has not been undertaken in earlier studies. Some studies focus only on power transmission enhancements [11,51–53], others on battery storage only [12,28,54,55], others on a combination of grid enhancement and battery storage [22,49,56,57], and others on a combination of geographical distribution and power transmission [20,58]. However, as pointed out by Heard et al. (2017), the criteria for simulating a reliable system with large VRE shares includes ensuring that any transmission requirements for newly installed capacity are described and geographically mapped and ensuring that critical ancillary services such as battery storage will be provided. To take advantage of the smoothening effect of transmission grid enhancement, it is essential to accurately model the geographical distribution of VRE power locations and to include an analysis of transmission grid effects on a higher time resolution and the integration of large-capacity battery storage.

This study, therefore, focuses on the effects of a combination of power fluctuation reduction measures including geographical distribution of VRE locations, power transmission enhancement, and introduction of battery storage. The main objective of this study is to determine the power supply mix

with large-scale solar PV and wind considering a combination of the power fluctuation reduction measures while minimizing the total power supply costs. The novelty and main contributions of this paper are as follows: (i) provide an effective method of integrating high shares of VRE at a lower total cost of power supply through a combination of the geographical distribution of VRE locations, transmission capacity enhancement, and the introduction of battery storage; (ii) identify the combination of power fluctuation reduction measures effective to achieve a particular share of VRE in the power supply system; and (iii) provide an analysis of the integration of VRE in the power supply system of Hokkaido, which can provide insight on the on-going commitment to increase the share of renewable energy in Japan.

The analysis considered Hokkaido, the northernmost prefecture of Japan, as a case study. Hokkaido is a cold region characterized by long, usually very cold winters, and short summers. The cold region climate offers large wind energy potential [59] with a high-power demand for heating. Wind and solar power generation, and power demand depend on the weather, and therefore the hourly, daily, and seasonal variability exhibited in cold regions needs to be accounted for in the energy system analysis [60,61]. The available literature on VRE integration in Hokkaido includes an investigation of the utilization factor of an electricity transmission network by determining the optimal installation of renewable energy technologies [22], and the development of an algorithm that identifies the most economically advantageous power source when solar and wind power stations are interconnected over a large area [62]. Therefore, this study adds to the knowledge of power systems in Hokkaido regarding the consideration of power fluctuation mitigation measures.

3.2 Methods

3.2.1 Model objective function

We developed a linear programming-based power supply optimization model with an objective function of minimizing the total annual cost of power supply while meeting the power generation conditions that are provided by constraint equations. The annual cost includes the annualized investment costs, operation and maintenance costs, and variable costs of the power supply facilities, power transmission lines, and battery storage facilities. The solution of the optimization model is a minimized total annual cost of power supply *(TCost)* is defined in Eq. (3.2.1).

$$min.TCost = \sum_{r=1}^{4} \left\{ \sum_{i=1}^{6} \left((\alpha_i IC_i + MC_i) P_{i,r} + \sum_{t=1}^{TD} VC_i E_{i,t,r} \right) + TC_r + SC_{s,r} \right\} \quad (3.2.1)$$

Where α_i is the annual capital cost recovery factor of power plant i; IC_i is the investment cost (JPY/kW) of power plant i; MC_i is the operation and maintenance cost (JPY/kW) of power plant i; VC_i is the variable cost (JPY/kWh) of power plant i; t is the time (hours), and TD is the total time in a year (8760 hours). The power plant lifespan is accounted for in the capital cost recovery factor α_i. The power transmission cost TC_r is defined in Eq. (3.2.2).

$$TC_r = (\alpha_T IC_T TL_r + MC_T) T_r + \sum_{t=1}^{TD} VC_T \left(T_{t,r}^{in} + T_{t,r}^{out} \right) \quad (3.2.2)$$

Where: α_T is the capital cost recovery factor, IC_T is the investment costs of power transmission capacity (JPY/kW/km), MC_T is the operation and maintenance cost (JPY/kW), and VC_T is the variable cost for power transmission (JPY/kWh), and TL_r is the length of transmission line r. The battery storage used in this model is the sodium sulfur (NaS) battery which has a power (kW) and an energy (kWh) component of its capacity. The battery storage cost $SC_{s,r,}$ is defined in Eq. (3.2.3).

$$SC_{s,r} = \sum_{s=1}^{1} \left(\left(\alpha_s^1 IC_s^1 PS_{s,r}^1 \right) + \left(\alpha_s^2 IC_s^2 PS_{s,r}^2 \right) + \sum_{t=1}^{TD} VS_s Cha_{s,r,t} \right) \quad (3.2.3)$$

Where: $\alpha^1{}_s$ is the annual fixed cost recovery factor for the power component of storage facility s, $\alpha^2{}_s$ is the annual fixed cost recovery factor for the energy component of storage facility s, $IC^1{}_s$ is the fixed cost of the power component of storage facility s (JPY/kW), $IC^2{}_s$ is the fixed cost of the energy component of storage facility s (JPY/kWh), and VS_s is the variable cost for materials such as electrodes and electrolytes (JPY/kWh).

Additional assumptions include;

- No minimum operation loads and no capacity factor constraints for LNGCC and LNGOC are considered. This is because the present model does not consider the numbers of LNGCC and LNGOC but considers only the capacities in each region. The LNGCC and the LNGOC are

assumed by a combination of several numbers of plants respectively, and very low loads may be possible. The installed capacity and capacity factors are endogenously determined from the optimization solution and are discussed in section 3.3.5.

- The installed capacity of hydropower plants is fixed with no provision for capacity increase.
- The excess power is discarded at the source and does not flow into the power transmission line. The techniques and costs of discarding excess wind and solar power are not considered. A detailed understanding of the effects of excess power management costs and the individual benefit to power producers is desirable and will be the focus of our subsequent studies.
- This study only focuses on the operation of a power system in the target year (2050) at an hourly time resolution (to elucidate the effects of VRE power fluctuations), and the timeline for the installation and decommissioning of power plants is not considered.
- Land constraints such as the availability of land area for the installation of renewable energy and conflicting usage of land for other purposes are not considered.
- Hokkaido Electric Power Company's power development plans are not considered.

3.2.2 Scenario description

In the analysis, four (4) scenarios (Case A, Case B, Case C, and Case D) with different combinations of power fluctuation mitigation measures are considered. Case A has no intervention constraints, Case B considers transmission capacity increases, Case C introduces battery storage, and Case D is a combination of transmission capacity increases and the introduction of battery storage. The scenarios are analyzed with the share of VRE increasing from 0 % to 80 % of the power supply required to meet the power demand. The VRE share is an input parameter while the power generation costs, installed capacities, and power output profiles are endogenous variables. Table 3.1 below describes the scenarios.

Table 3.1. Combination of power fluctuations mitigation measures in the four scenarios.

	Case A	Case B	Case C	Case D
Geographical Distribution of VRE sites	✓	✓	✓	✓
Transmission Capacity Increase	✗	✓	✗	✓
NaS batteries Introduction	✗	✗	✓	✓

3.3 Results and discussion

Employing the optimization model described in section 2.1.1, this study estimates the annual cost of power generation, the power output profiles, and the installed capacities of power supply technologies for different scenarios which have varying combinations of power fluctuation mitigation measures. The authors perform an analysis to evaluate the economic competitiveness of combining the geographical distribution of candidate VRE power locations, the enhancement of transmission capacities, and the integration of battery storage in the power supply system of Hokkaido. To simplify the discussion of the results, the authors introduce three tiers of VRE share. Each tier represents a range of VRE shares within which the effects of power fluctuation measures are distinguishable. The first tier represents a share of VRE from 0 % to 40 %, the second tier is the VRE share from 40 % to 60 %, and the third tier is the VRE share from 60 % to 80 %. In this study, VRE share refers to the ratio of power supply from wind and solar PV in the total power demand. The VRE share does not include excess power generation, which is not utilized in meeting the power demand. The results are categorized into three tiers to substantiate the effectiveness of power fluctuation reduction measures that vary differently in each tier as will be discussed below.

3.3.1 Annual power supply cost

The total annual power supply costs and the components of the costs are illustrated in Fig. 3.1 and Fig. 3.2, and the power supply and demand are shown in Fig. 3.3. The total annual power supply cost shows no increase in the first tier (0 ~ 40 %), while a significant increase is observed in the second tier (40 ~ 60 %) and third tier (60 ~ 80 %) of VRE share. Figures 3.1 and 3.2 suggest that up to 40 % VRE share can be achieved by geographically distributing the VRE locations. As the total annual power supply cost of Cases B, C, and D are similar to that of Case A in tier 1, the increase in the transmission line capacity and the introduction of battery storage does not significantly reduce the total power supply cost. In the second tier of VRE share (40 % to 60 %), increasing the power transmission capacity plays a significant role in minimizing the total annual power supply cost, while the introduction of battery storage is more effective in reducing the total power supply costs in the third tier (60 % to 80 %). Overall, the results show that combining the three power fluctuation measures has more economic advantage in the integration of VRE in the power supply system. Details of the effects of each of the measures for VRE power fluctuation reduction are discussed in the subsequent sections.

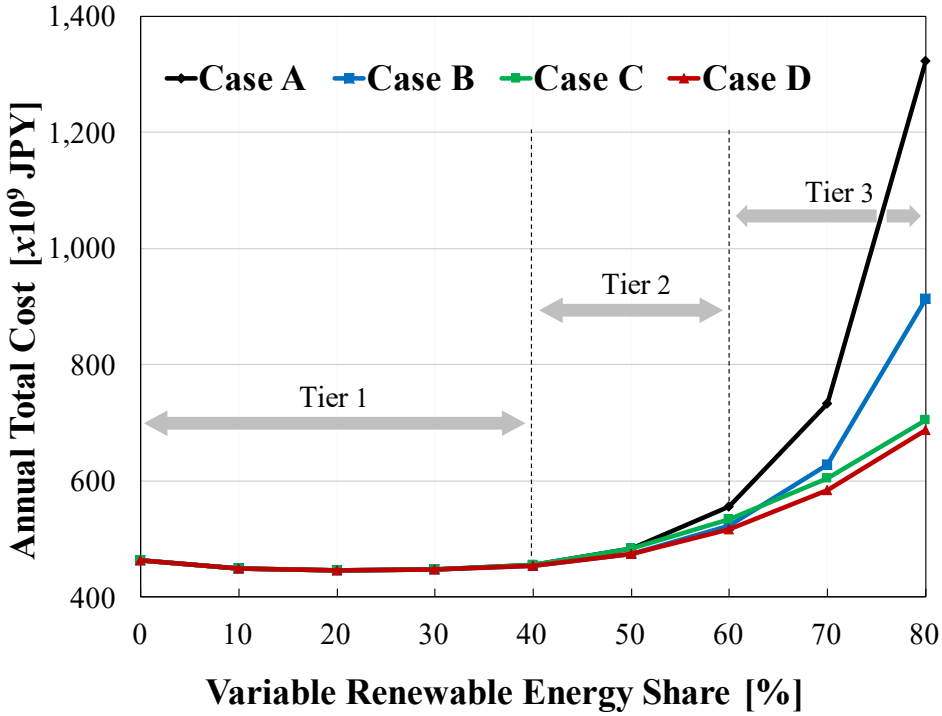

Fig. 3.1. Variation of Total annual power supply costs (JPY) with increasing VRE share for all the scenarios considered here.

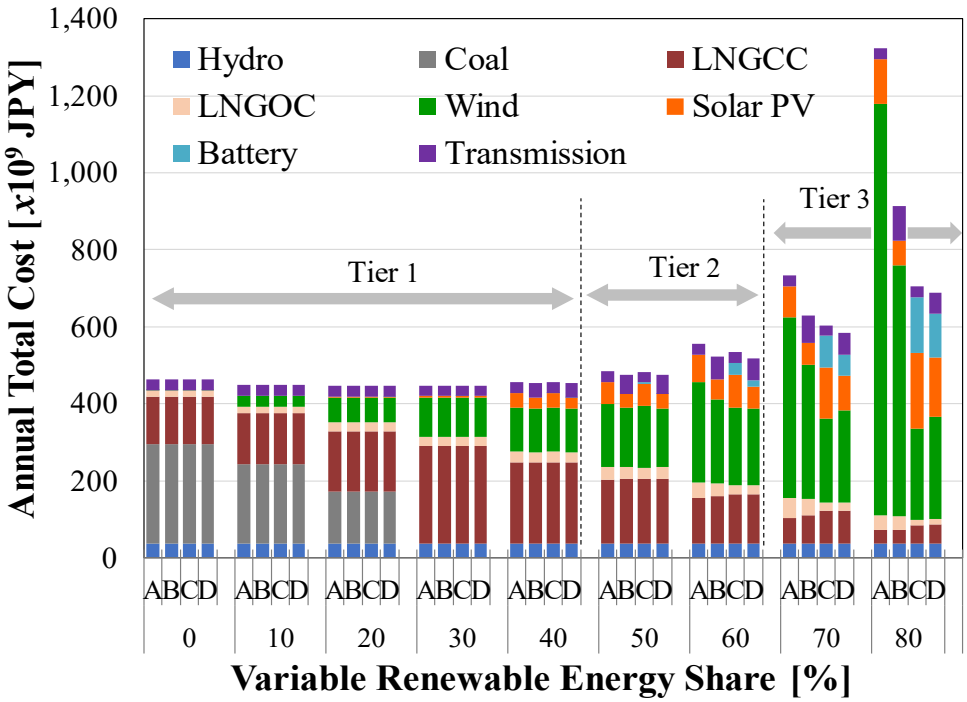

Fig. 3.2. Variation of the eight components of the total annual power supply cost (JPY) by Case and VRE share.

Further, excess power supply, which is represented by the amount of power supply above the power demand (black dotted line in Fig. 3.3), is insignificant in the first tier (0 ~ 40 %) and increases in the second and third tiers (> 40 %). From 30 % VRE share, the thermal power supply from coal power generation is replaced by wind and LNGCC thermal power. The power supply is similar for all the scenarios in the first tier, but large variations can be observed in the second and third tiers (> 40 %).

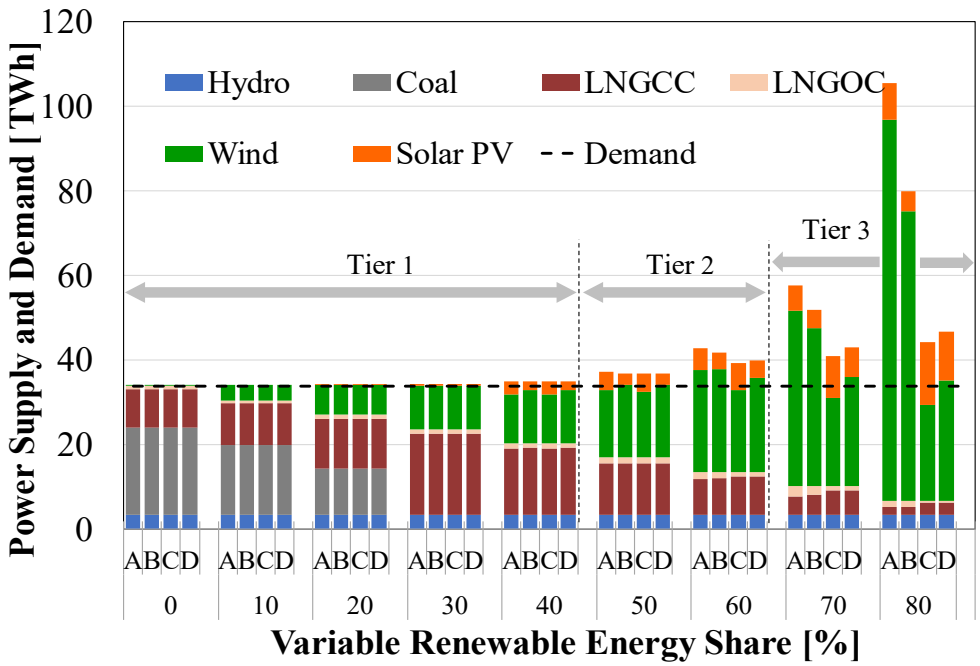

Fig. 3.3. Power supply components (TWh) and power demand (TWh) by Case and VRE share.

3.3.2 Geographical distribution of VRE locations

As shown in Figs. 3.1 and 3.2, the annual power supply costs for all the scenarios in the first tier of the VRE share (0 ~ 40 %) are comparable. Introducing wind and solar PV power results in a slight reduction in the cost of the power supply, and the utilization of coal thermal power which has a constant power output is reduced. As discussed in section 3.3.3 below, there is no increase in the capacity of transmission lines and the introduction of battery storage is not in effect in the first tier so the suppression of the increase in the cost of power supply and the generation of excess power is achieved due to the location distribution of wind and solar PV power sites. The power supply system operates such that during periods of low power supply in one location, surplus power supply from another location compensates for the low supply through the power transmission lines. The transmission of

power among the different locations suppresses excess power generation and thus minimizes the increase in the total cost of the power supply.

Figure 3.4 shows the sites where wind and solar PV power installation occurs among the candidate locations and the installed capacities in the first tier (<40 %) for Case A (which are similar to Cases B, C, and D). The installed capacity is color-coded for each region. Blue is the central region, red is the southern region, green is the northern region, and purple is the eastern region of Hokkaido. Locations (1), (4), and (5) are for solar PV power, and the others are for wind power. The central region with the high-power demand has the highest installed capacity for wind and solar PV power. The provision of candidate sites for the installation of wind and solar PV enables the selection of the most suitable sites in a way that reduces the generation of excess power and limits the increase in the cost of power supply. For a 10 % VRE share, only 3 wind power sites are selected whereas for a 40 % VRE share 6 wind power and 3 solar PV sites are selected.

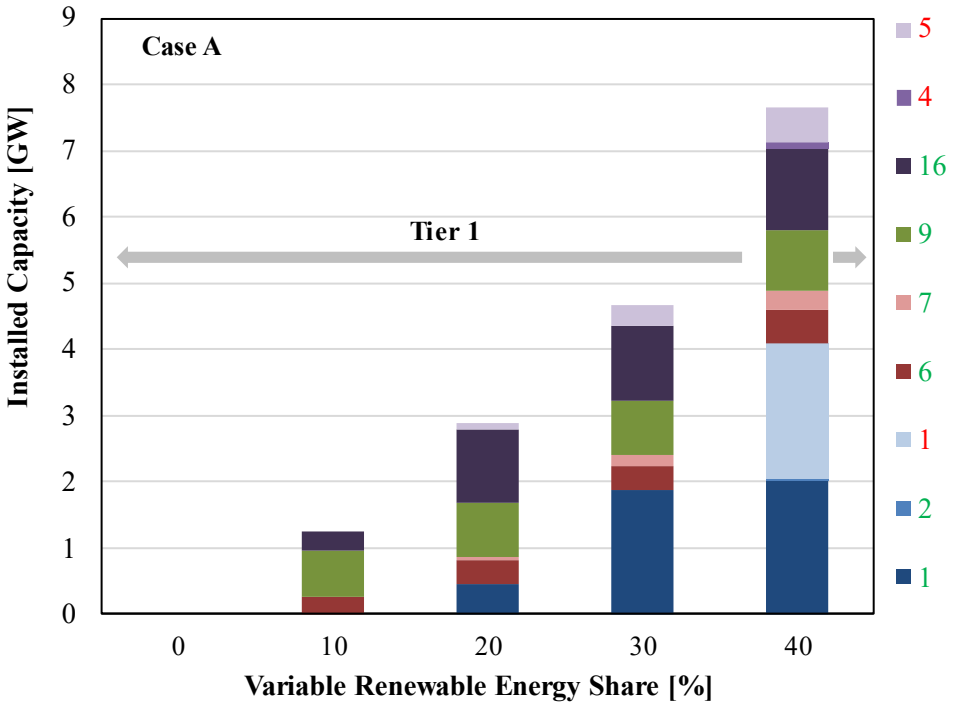

Fig. 3.4. Wind and solar power installed capacity (GW) in the selected locations for Case A.

To optimize the cost of power supply, some sites are selected from the candidate locations depending on the VRE share. While the capacities of the selected sites vary depending on the VRE share, the total power supply cost remains fairly constant as VRE power replaces the thermal power

sources (Coal, LNGCC, and LNGOC) which have relatively higher running costs. The results for Case A being similar to that of Cases B, C, and D, suggest that the current power transmission capacity as shown in Fig. 2.1, and the geographical locations of the selected sites are sufficient for the integration of up to 40 % VRE share without introducing battery storage. Therefore, there is no need to increase the power transmission capacity and introduce battery storage to achieve up to 40 % VRE share in Hokkaido's power supply system.

Further, there is a relationship between the existing power transmission line capacity and the power demand in each region, and the capacity of the VRE installed in each region. At the 40 % share of VRE, the capacity of wind power installed in the northern region (0.8 GW) is equivalent to the sum of the power transmission capacity of 0.4 GW and the average power demand in the region (0.4 GW). Similarly, in the eastern region, the capacity of wind power installed (1.2 GW) is equivalent to the sum of the power transmission line capacity (0.6 GW) and the average power demand (0.6 GW). To achieve the VRE in the first tier (Fig. 3.4), the actual installation is only needed in selected sites and the installed capacities are relative to the power transmission line capacity and the average power demand in each region. This relationship observed here is due to the constraint of the power transmission capacity such that the amount of wind power installed does not exceed the amount required to meet the local demand and the amount to be transmitted to the other regions through the power transmission lines.

Figure 3.5 shows the power generation profile for January on an hourly interval at the 40 % VRE share in the central and northern regions for Case A. In the northern region, the wind power output has a constrained maximum of 0.8 GW, which is similar to the sum of the average power demand at 0.4 GW, and the power output transmitted to the central region is constrained at a maximum of 0.4 GW which is the transmission capacity of the Central-North line. Due to power fluctuations of wind and solar PV, there is surplus power output in both regions. However, the amount of surplus power supply is the smallest in the central region with the higher power demand. In the northern region, the amount of wind power supply compared to the power demand is much higher, and therefore a large amount of surplus power is produced. This surplus power is transmitted to the other regions to minimize power wastage. The current transmission capacity absorbs the power fluctuations and reduces power wasted in the first tier due to the geographical distribution of the location of the VRE sites.

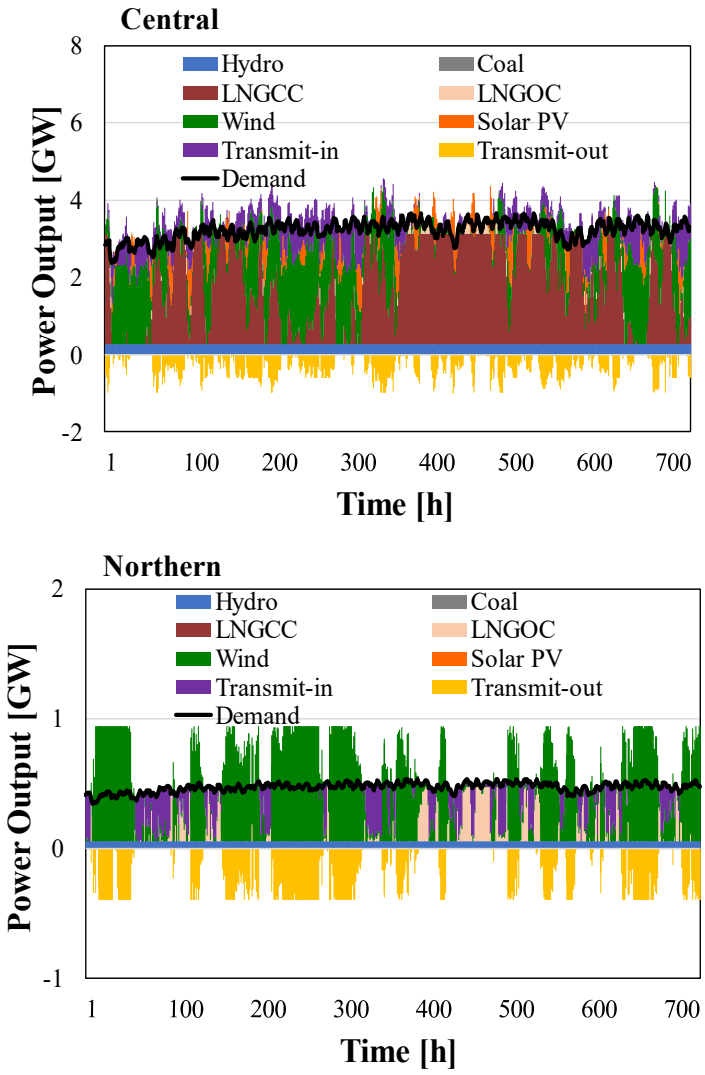

Fig. 3.5. Power Generation profile for January on an hourly interval at the 40 % VRE share in the northern and central regions for Case A.

3.3.3 Increase in transmission line capacity

Figure 3.6 shows the increase in the power transmission capacity with an increase in the VRE share for Case B (without battery storage) and Case D (with battery storage). In the second tier, there is an increase in the central-northern transmission capacity from 0.98 GW at 40 % to 2.2 GW at the 60 % VRE share for Case B while the central-eastern and central-southern lines have no increase in the transmission capacity. In Case D, the increase in the central-northern transmission capacity is similar to that of Case B. The variation in the transmission line capacity in tier 3 is explained in section 3.4.

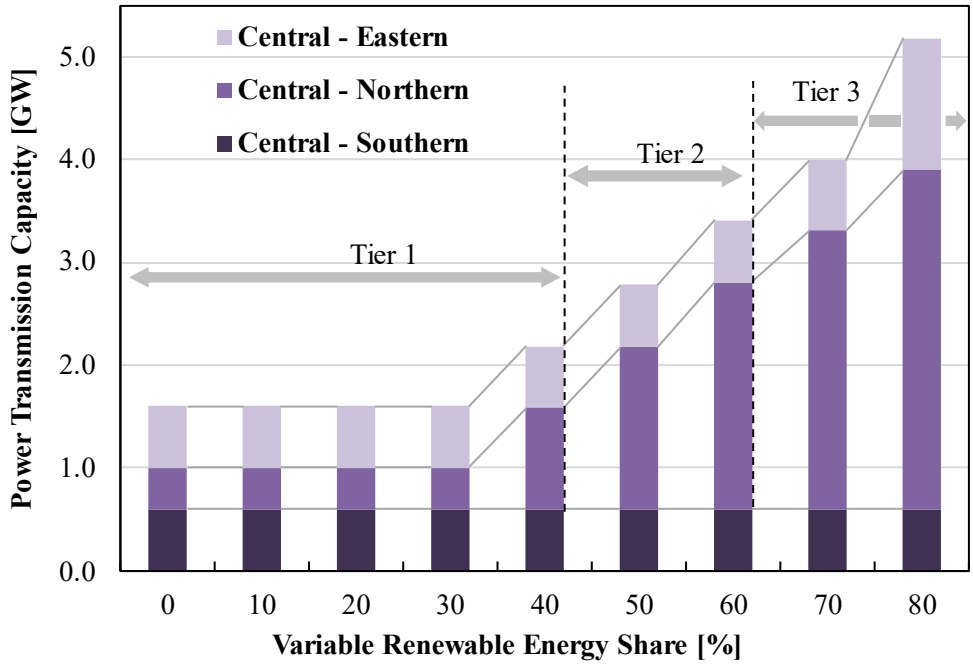

Case B Transmission enhancement (without battery storage)

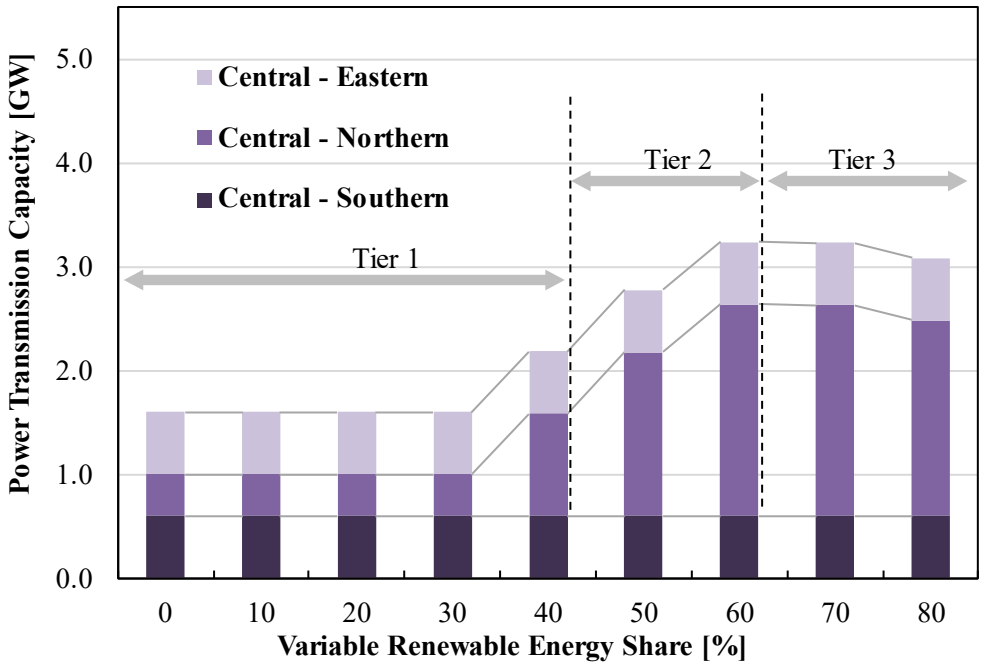

Case D Combined transmission enhancement and battery storage

Fig. 3.6. Increase in power transmission capacity (GW) with increasing VRE share for Case B (without battery storage) and Case D (with battery storage).

As observed in Fig. 3.1 in the second tier (40 % ~ 60 %), increasing the transmission capacity (Case B) has an economic advantage over the introduction of battery storage (Case C). The increase in the central-northern transmission line capacity facilitates the transmission of surplus power from the north to the other regions through the central region. The introduction of battery storage has minimal effect on the suppression of the increase in the power supply cost as well as in reducing the surplus power generation. Therefore, for the second tier VRE share (40 % ~ 60 %), only an increase in transmission capacity is sufficient to minimize the total cost of power supply and the introduction of battery storage is not necessary.

3.3.4 Introduction of battery storage

As shown in Fig. 3.1 and Fig. 3.2, there is a significant increase in the power supply cost in the third tier of VRE share (60 % to 80 %). The introduction of battery storage (Cases C and D) is more effective in reducing the cost of the power supply and the generation of surplus power in the third tier than in the first and second tiers. Further, the introduction of battery storage reduces the increase in the transmission line capacity as shown in Fig. 9. In Case B, the transmission capacity for the central-north transmission line increases from 2.22 GW at 60 % to 3.29 GW at 80 %, and the central-eastern line capacity increases from 0.60 GW at 60 % to 1.30 GW at 80 %. In Case D, the capacity of the central-north line reaches its maximum capacity of 2.04 GW at the 60 % VRE share and reduces to 1.93 GW at the 80 % VRE share.

The results observed in Fig. 3.6 suggest that the introduction of battery storage reduces the need for higher power transmission capacities. In addition to battery storage reducing the amount of power discarded and the cost of power supply, the results show a correlation between battery storage and the share of solar PV introduced in the power supply mix. As noted in Fig. 6, where Cases C and D have a higher power supply of solar PV than Cases A and B, introducing a large battery storage capacity enables the integration of high shares of solar PV power in the power supply mix.

Figure 3.7 shows the power supply and storage installed capacity in Cases C and D. In Case C without provision for increases in transmission capacity, achieving 80 % VRE share requires the installation of a larger amount of VRE in the central region which has a larger power demand. For Case D, with increases in transmission capacity and battery storage, the capacity of power generation and storage facilities in the central region is less than that in Case C. Introducing battery storage and

increasing the transmission capacity facilitates the installation of larger capacities of wind power in the northern region as suggested by Fig. 3.7. The capacity of battery storage introduced in each region depends on the capacity of wind and solar PV installed.

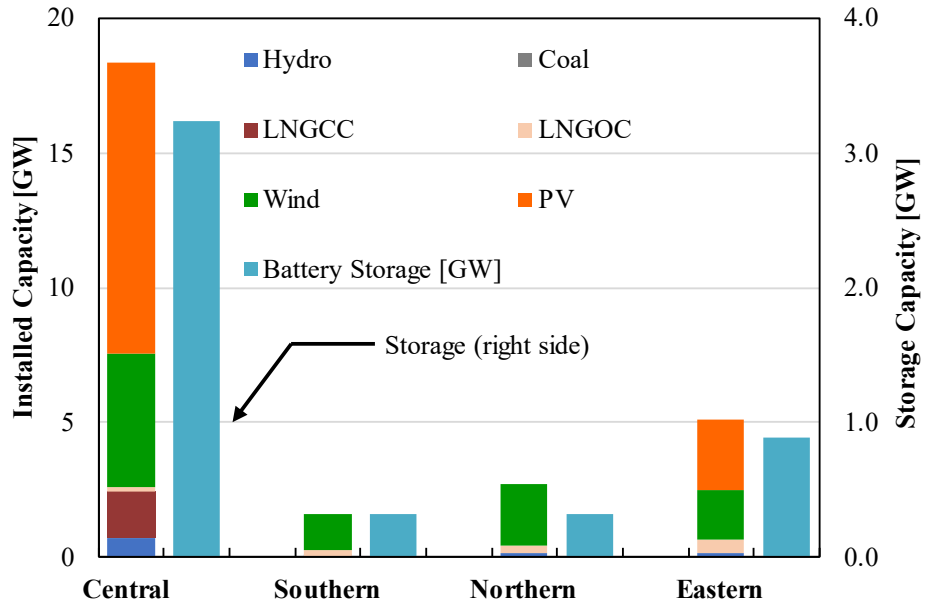

(a) Case C (without transmission capacity increase)

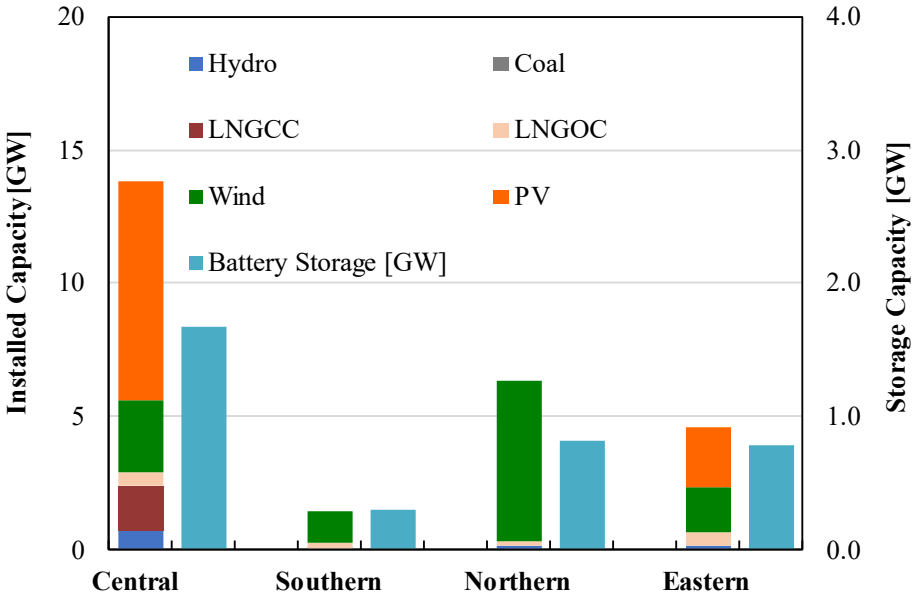

(b) Case D (with transmission capacity increase).

Fig. 3.7. Power supply and battery storage installed capacity at the 80 % VRE share for (a) Case C (without transmission enhancement) and (b) Case D (with transmission enhancement).

Further, Fig. 3.8 shows the power output for Case C and Case D in the third tier (60 % to 80 %). In the figures, Local refers to the amount of power that is consumed within the region where it is produced, Trans-out refers to the amount of power transmitted to the other regions, and Excess refers to the amount of power that is discarded in each region. Surplus power in each region is equivalent to the sum of the power transmitted to other regions and the excess power. Without provisions for increases in power transmission capacity, the surplus power is the largest in the central region for Case C due to the larger capacities of wind and solar PV and the amount of wind power generation in the northern region is less than that obtained in Case D which has provisions for increases in transmission capacity and introduction of battery storage.

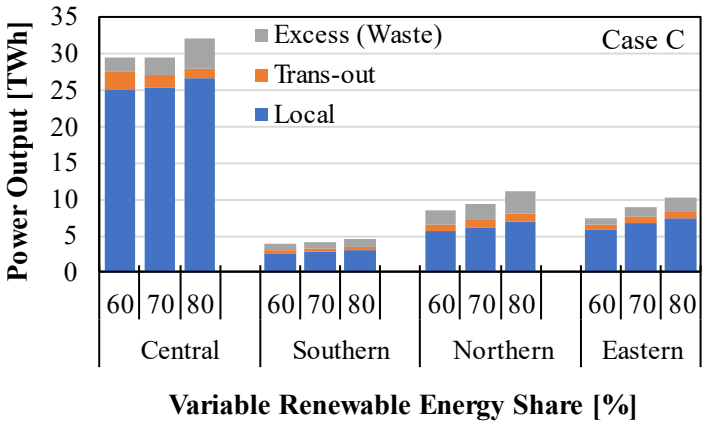

(a) Case C (without transmission capacity increase)

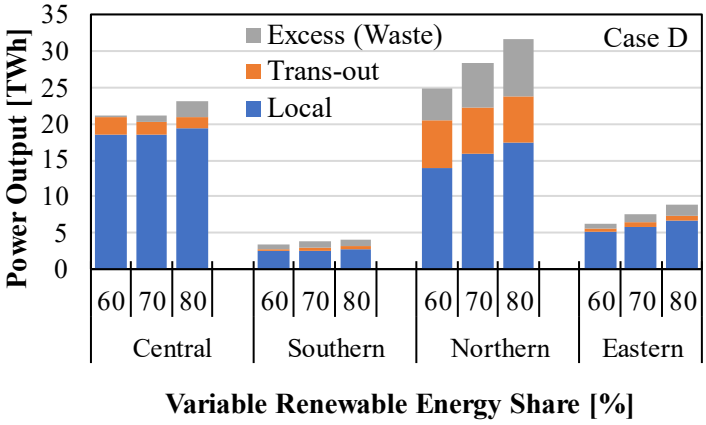

(b) Case D (with transmission capacity increase).

Fig. 3.8. Total power output from 60 % to 80 % VRE share for all the regions. (a) Case C (without transmission capacity increase) and (b) Case D (with transmission capacity increase).

Figure 3.9 shows the power generation profile for January at 80 % (a) in the central and northern regions for Case B VRE share, and (b) in the central region for Cases C and D. It is observed from Fig. 12 that the amount of surplus power, represented by power output above the power demand (black line), is less in the central region which has a large power demand. In the northern region, the increase in power transmission facilitates a large amount of wind power generation and this results in significantly large surplus power generation, part of which is transmitted to the other regions through the central region. With the introduction of battery storage (Case C), a large amount of solar PV power is added to the central region than in Case B which only has power transmission capacity increases. The combination of the two power fluctuation mitigation measures (Case D) shows a reduction in the amount of excess power and an increase in the amount of power transmitted into the central region from other regions.

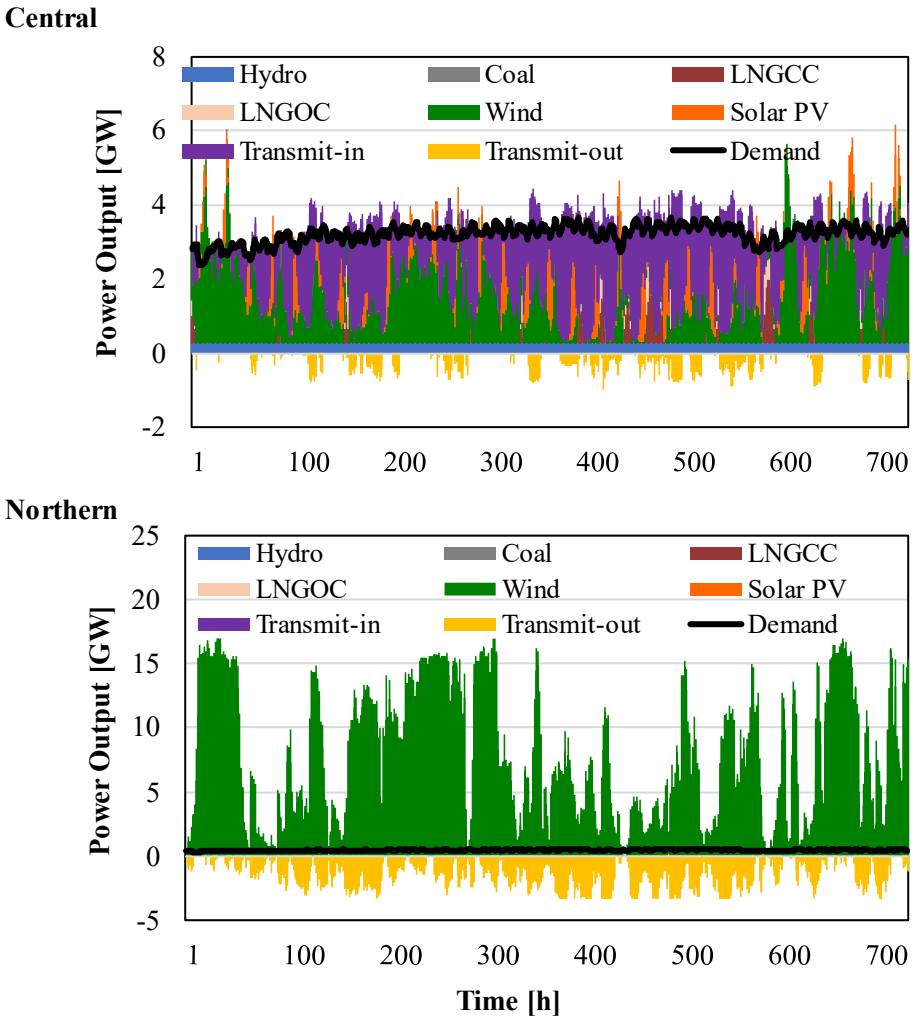

(a) Central and northern regions for Case B

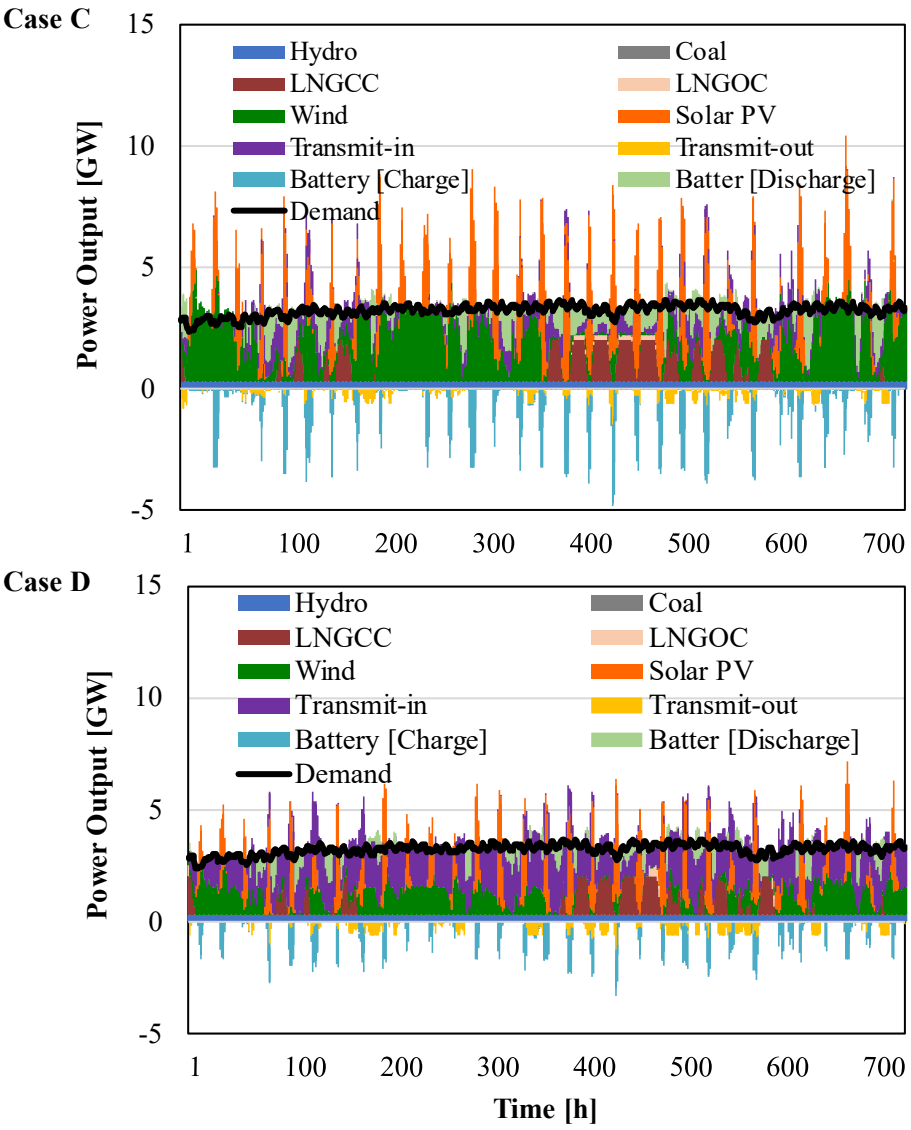

(b) Central region for Cases C and D

Fig. 3.9. Power Generation profile for January on an hourly interval at the 80 % VRE share. (a) Central and northern regions for Case B and (b) Central region for Cases C and D.

3.3.5 Cross-cutting issues

Excess power generation cannot be avoided due to the unpredictable fluctuations of wind and solar PV power as suggested by Fig. 2.2. The measures discussed above need to be integrated with the development of large-scale VRE to reduce excess power generation. This analysis has shown that there is a large amount of excess power generated in the second and third tiers (>40 %). Figure 3.10 shows

the effect of the increase in excess power generation on the total annual cost of power supply for all four scenarios. Excess power from VRE increases the total cost of the power supply and the rate of increase in the cost of the power supply varies in each of the scenarios. Without power fluctuation mitigation measures, there is a high increase in the total cost of power supply with an increase in excess power. The increase in the power transmission capacity and the introduction of battery storage reduces excess power and the cost of power supply. Compared to the introduction of battery storage, combining battery storage and transmission capacity enhancement has a lower increase in power supply cost. In this analysis, large amounts of excess power at high VRE shares are discarded and this can potentially increase the cost of power supply to cover the cost of power discarding equipment, resulting in high prices of electricity from VRE sources. However, excess power has potential applications in other sectors such as the transport sector for charging electric vehicles (EV) as well as for hydrogen production to use in hydrogen-driven vehicles. In addition, while the effects of the Hokkaido-Honshu HVDC power interconnector on the Hokkaido power system are not considered in this analysis, the interconnector provides a way to transmit the excess power from Hokkaido to the other parts of the country.

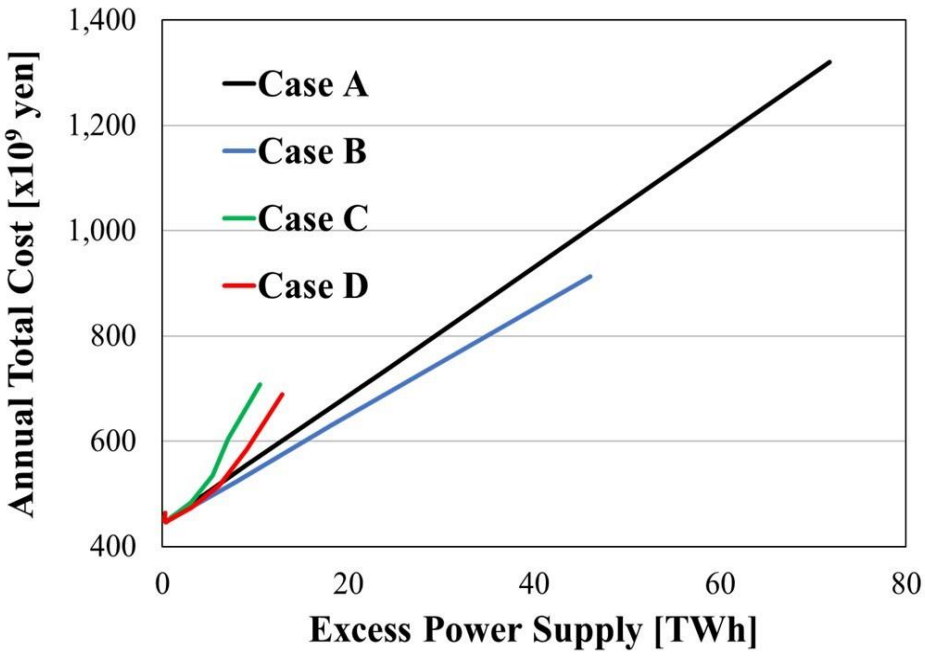

Fig. 3.10. Variation of the total annual power supply cost (JPY) and excess power supply (TWh).

Figure 3.11 shows the capacity factor (%) and installed capacity (GW) for LNGCC and LNGOC thermal power for the combined measures scenario (Case D). The LNGCC has a higher capacity factor than LNGOC. While the capacity factor for LNGOC does not change significantly with the increasing share of VRE, the capacity factor for LNGCC significantly reduces with increasing VRE share. Similarly, the installed capacity of LNGCC peaks at 3.0 GW at the 30 % VRE share and then decreases with an increase in the VRE share. The LNGOC installed capacity reaches a maximum of 2.0 GW at 50 % VRE and thereafter decreases. Figure 14 suggests that for Hokkaido's power system with a low VRE share, increasing the installed capacity and capacity factor of natural gas thermal power is necessary to replace coal thermal power. At higher VRE shares the installed capacity and capacity factor for natural gas thermal power decreases. However, despite the decrease in utilization, the load-following thermal power cannot be eliminated from the power supply system as thermal power is needed to provide backup power when wind and solar PV power fluctuates below the power demand. A combined heat and power thermal backup system may also be a good candidate to effectively utilize the excess power for both heat and electricity production.

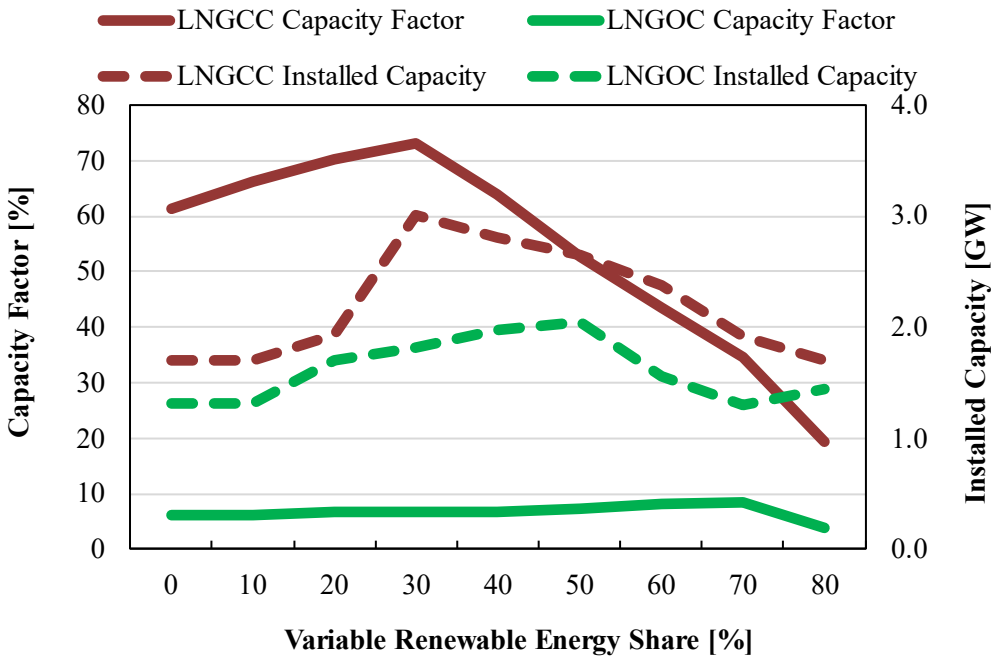

Fig. 3.11. Back-up thermal power capacity factor (%) and installed capacity (GW) with increasing VRE share for Case D.

3.4 Conclusions of chapter 3

In this study, we considered the separate and combined effect of the geographical distribution of VRE locations, enhancements of power transmission capacity, and the introduction of battery storage on the integration of high VRE shares in the power supply system. The analysis was applied to Hokkaido as a case study. From the results we can conclude that;

- The combination of the geographical distribution of VRE locations, transmission capacity enhancement, and the introduction of battery storage, is the most economical way of integrating VRE in power supply systems. The effects of the combination of these three measures on the reduction of excess power generation and the reduction in the power supply costs outweigh that of individual effects or that of a combination of only two of these measures. To effectively increase the VRE share in a power supply system, careful consideration should be made for the geographical location of VRE sites and provisions should be made to upgrade the transmission capacity and introduce battery storage.

- To identify the combination of power fluctuation reduction measures effective to achieve a particular share of VRE in the power supply system, this study reveals that by geographically distributing the locations of VRE sites, up to 40 % VRE share can be achieved without upgrades to the power transmission and storage capacities. Therefore, it is important to optimize the location of solar and wind power generation sites through the selection of suitable sites from candidate sites. For the second tier of VRE share (40 % to 60 %), an increase in the transmission capacity coupled with VRE geographical distribution is needed to minimize the excess power generation and the total power supply cost. For VRE from 60 % to 80 %, the introduction of battery storage in addition to enhancements in transmission capacity provides an effective option for reducing excess power generation and minimizing the cost of power supply.

- The introduction of battery storage facilitates the integration of a larger capacity of solar PV power while transmission enhancement enables the integration of larger capacities of wind power.

- Applying the measures above still leaves a level of excess power generation increasing from the 60 % VRE share. However, excess power has potential applications in other sectors such as charging electric vehicles (EV) and hydrogen production for hydrogen-driven vehicles in the

transport sector. While these applications can significantly reduce the discarding of excess power, it is not certain if the discarding of power can be eliminated in power systems with high VRE shares. Further, the HVDC interconnection with the Honshu region also provides an avenue for the transmission of excess power from Hokkaido to the Honshu region.

- Additionally, a thermal backup system such as combined heat and power (CHP) may be a good candidate to mitigate costs incurred by the fluctuations. For heat supply, a heat pump system utilizing surplus power can also be integrated. The system would have the potential to effectively utilization of surplus power due to the utilization of both electricity and heat for various applications such as space heating during winter.

4 Chapter 4: Analysis of electricity prices for power supply toward a social optimum for installed wind and solar power utilization

4.1 Introduction

The 2015 Paris Agreement set the ambitious goal of limiting global warming to well below 2°C compared to pre-industrial levels through the reduction of greenhouse gases (GHG) [2]. The development of variable renewable energy (VRE), which includes wind and solar photovoltaic (PV) sources, is an effective way to reduce GHG emissions in the power sector. With supporting policies such as a feed-in tariff (FIT) policy, VRE installation has increased significantly over the years. At the end of 2021, VRE dominated renewable capacity expansion and accounted for 88 % of all renewable energy capacity additions [63]. During the period from 2010 to 2021, there has been a significant increase in the competitiveness between VRE and conventional fossil fuel options. The global weighted average levelized cost of electricity (LCOE) of utility-scale solar PV projects declined by 88 % during the period, whilst that of onshore wind declined by 68 %. The capacity factors of wind and solar PV have increased during the period from 27.2 % to 39.2 % for wind, and from 13.8 % to 17. 2 % for solar PV [64]. This reduction in installation costs, capacity factors, and LCOE are key factors contributing to the expansion of VRE. As VRE development continues to increase, the effective integration of high shares of VRE in power supply systems needs to be carefully considered.

While the increased deployment of VRE plays a key role in the reduction of carbon dioxide (CO2) emissions in the power sector and the transition to a low-carbon energy system. However, the integration of VRE into power supply systems offers specific challenges due to intermittency, non-dispatchable feature, and uncertainties in energy output. The power output fluctuations associated with high VRE shares require measures such as considering the geographical distribution of VRE locations, integration of battery storage, power transmission capacity enhancement, and demand-side management [10–13]. Studies have shown that the geographical distribution of interconnected VRE power supply reduces the effects of fluctuations in that the fluctuations of one region are offset by the output of another region. This significantly reduces the need for battery storage and backup thermal power sources required to stabilize the supply of electricity [14]. The integration of battery storage systems has been determined to facilitate smoothening of the power output from VRE power and to decrease the mismatch between power supply and demand [15,16]. Integrated battery storage systems play a significant role in realizing high VRE shares in power supply systems. Further, the enhancement

of power transmission lines enables access to areas of high VRE potential. The interconnection of VRE reduces the need for battery storage and backup thermal power supply [17].

The aforementioned power fluctuation reduction measures enable the integration of high shares of VRE in the power supply system, maintain the stability of the system, and improve the quality of the power supply. The improvement in power technologies, coupled with the decline in installation costs has led to an increase in the VRE installed capacities. Further, there has been an upward trend in the share of VRE electricity. The large-scale purchase of VRE electricity has largely been sustained by supporting policies such as the feed-in tariffs (FIT) policy. The FIT policy was designed to stimulate VRE investments by guaranteeing the long-term purchase of electricity [65–67]. Feed-in tariffs have been pivotal in accelerating the deployment of VRE and remain the dominant form of policy support for VRE power generation. However, after phasing out of such policies, the deployment of VRE power will mainly depend on the competitiveness of the VRE electricity prices relative to other power supply sources. The continued decline in VRE investment costs will enable the transition to competitiveness for VRE electricity. Power system modeling provides the tools for analyzing power supply electricity prices towards the utilization of integrated VRE power sources.

Power supply system modeling is the systematic forecasting of the power supply and power demand based on changes in specific conditions. Modeling of power supply systems with large-scale VRE must ensure the proposed electricity supply is capable of meeting the electricity demand. At the same time, the power supply system model should aim at minimizing the effects of VRE power output fluctuations. . The literature on power supply system modeling covers various aspects including the development of models for the integration of renewable energy [58,68,69], and using models to explore the transition from fossil-based to the feasibility of 100 % renewable energy-based power systems [49,50,55,57,70]. In our previous study [10], we developed a power supply optimization model to examine the effects of power fluctuation mitigation measures including geographical distribution on the integration of large-scale VRE in power supply systems. The target of the objective function was the total cost of the power supply. The optimization model minimized the total cost of power supply which included the investment, operation and maintenance, and variable costs. Using the model, we were able to determine the power output profiles and the minimized power supply cost.

The above-mentioned studies are total system optimization models. Total system optimization modeling has been used extensively to determine what an optimum total power supply system should

be comprised of under specified conditions. However, actual power supply systems are developed by the partial optimization of various components of the entire system, such as the power supply, power transmission and distribution, and power demand components. The total optimization model in our previous study [10] can determine the optimum power supply installed capacity mix for a specified share of VRE in the power supply. However, the actual amount of VRE electricity in the power supply depends on the prices at which the power transmission and distribution (PTD) company purchases electricity from thermal and VRE power generation companies. Therefore, a partial optimization analysis of the PTD company is necessary to elucidate the effect of electricity prices toward an optimum social cost and VRE utilization.

The objective of this present study is to determine effective pricing conditions for increasing the share of VRE electricity in the power supply to meet the power demand. A linear programming-based partial optimization model is developed with the objective function targeting the cost to the PTD company. The optimization model minimizes the cost to the PTD company, which includes the cost of electricity purchase from power generation companies and the cost of installation and maintenance of battery storage and power transmission systems. This study provides the effective electricity prices necessary for the PTD company to achieve a power supply VRE share that is similar to that determined through the total system optimization approach. The main contributions of this paper include: (i) developing a partial optimization model to increase the integration of VRE in the power supply system; (ii) providing effective pricing conditions for achieving high VRE shares; (iii) increasing the integration of VRE electricity in the power supply system of Hokkaido through the partial optimization by the PTD company.

4.2 Methods

This study builds on the previous study by the author [10] which used a total system optimization approach to determine the power supply mix integrated with a large-scale VRE share in the power supply. The installed capacities of the power supply, battery storage, and transmission lines were optimized in the total system optimization model. This present paper focuses on partial optimization by the PTD company. Power supply options include hydro, coal, natural gas combined cycle (LNGCC), wind, and solar PV. The installed capacity of hydro, coal, and VRE power is fixed while the capacities of LNGCC, battery storage, and transmission lines are optimized in the partial optimization model. Figure 4.1 illustrates the power supply system with battery and transmission under the PTD company.

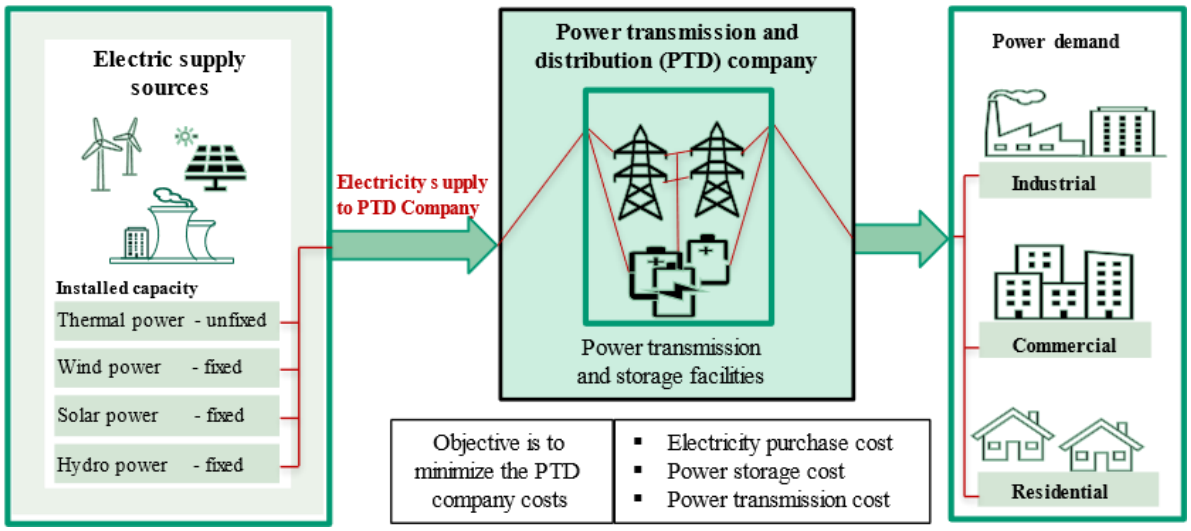

Fig. 4.1. Power supply system with the battery and transmission facilities under the PTD company.

4.2.1 Model objective function

The authors developed a linear programming-based partial optimization model to use for this analysis. The objective function is to minimize the cost for the PTD company, while the objective function in the previous study (Lukwesa et al., 2022) is the total cost of power supply. In the present study, it is assumed that the PTD company covers the cost of the installation and operation of the power transmission and storage facilities. Therefore, the cost to the PTD company includes the cost of purchasing electricity from power suppliers and the cost of installation and maintenance of energy storage and transmission facilities. The solution to the objective function (APCost) is defined by Eq. (4.2.1).

$$min.\,APCost = \sum_{r=1}^{4}\left\{\left(\sum_{i=1}^{4}\sum_{t=1}^{TD} ElP_i\, E_{i,t,r}\right) + SC_{s,r} + TC_r\right\} \tag{4.2.1}$$

Where ELP_i is the price of electricity (JPY/kWh) from the power generating source i; t is the time (hours), and TD is the total time in a year (8760 hours). The costs of setting up and maintaining the power transmission TC_r and battery storage $SC_{s,r}$ facilities are defined by Eqs. (4.2.2) and Eq. (4.2.3).

$$SC_{s,r} = \sum_{s=1}^{1}\left(\left(\alpha_s^1\, IC_s^1\, PS_{s,r}^1\right) + \left(\alpha_s^2\, IC_s^2\, PS_{s,r}^2\right) + \sum_{t=1}^{TD} VS_s\, Cha_{s,r,t}\right) \tag{4.2.2}$$

Where: α^1_s is the annual fixed cost recovery factor for the power component of storage facility *s*, α^2_s is the annual fixed cost recovery factor for the energy component of storage facility *s,* IC^1_s is the fixed cost of the power component of storage facility *s* (JPY/kW), IC^2_s is the fixed cost of the energy component of storage facility *s* (JPY/kWh), and VS_s is the variable cost for materials such as electrodes and electrolytes (JPY/kWh).

$$TC_r = (\alpha_T \, IC_T TL_r + MC_T) \; T_r \; + \sum_{t=1}^{TD} VC_T \left(T_{t,r}^{in} + T_{t,r}^{out}\right) \tag{4.2.3}$$

Where: α_T is the capital cost recovery factor, IC_T is the investment costs of power transmission capacity (JPY/kW/km), MC_T is the operation and maintenance cost (JPY/kW), and VC_T is the variable cost for power transmission (JPY/kWh), and TL_r is the length of transmission line *r*. The battery storage used in this model is the sodium sulfur (NaS) battery which has a power (kW) and an energy (kWh) component of its capacity.

In addition to the above equations, the model has constraint equations on the energy balance, power supply, storage, and transmission installed capacity constraints, and constraints on power supply capacity factors. To avoid repetition, the detailed description of the rest of the partial optimization model is similar to the total optimization model presented in section 2.1.1.

4.3 Results and discussion

4.3.1 Total system optimization

In our previous study [10], a power supply optimization model (referred to as the total optimization model in this study) was developed and applied to determine the optimum power supply cost and installed capacity mix for a specified VRE share. The VRE share refers to the amount of electricity from VRE sources in the power supply to meet the power demand. To optimize the power supply cost, VRE power fluctuation mitigation measures including the geographical distribution of VRE locations, battery storage introduction, and transmission capacity increases are considered. The power supply options in the previous study include hydro, coal, LNGCC, LNGOC, wind, and solar PV. In this study, LNGOC is not included in the power supply options as it does not significantly change the results of

the total optimization analysis. Therefore, this study first presents the total system optimization analysis results without LNGOC. The results at an 80 % VRE share will be used in the following partial optimization analysis.

The results of the total optimization model analysis are presented in Fig. 4.2. The obtained power supply mix without LNGOC was similar to that in our previous study with LNGOC (Case D). Figure 4.2 (a) shows the annual total power supply cost, which includes the costs of power generation, storage, and transmission, which is minimized at a specified VRE share. The results indicate that under the total system optimization, up to a 40 % VRE share is achievable with no increase in the power supply cost. However, with higher VRE shares (40 ~ 80 %), the total power supply cost increases due to an increase in VRE power supply. Figure 4.2 (b) shows the components of the power supply cost. When VRE power is not considered (0 %), the total power supply cost mainly consists of hydro, coal, LNGCC, and power transmission costs. When the VRE share is increased, LNGCC replaces coal as the backup thermal power up to a 30 % VRE share, followed by a decrease in the LNGCC cost up to 80% VRE share. The increase in the VRE share from 30 to 50 % is associated with an increase in transmission costs without an increase in battery costs. The geographical distribution of the VRE locations and the increase in transmission capacity contribute to suppressing the total cost [10]. Further, in Fig. 4.2 (b), high VRE shares (60~80 %) are associated with an increase in battery storage costs.

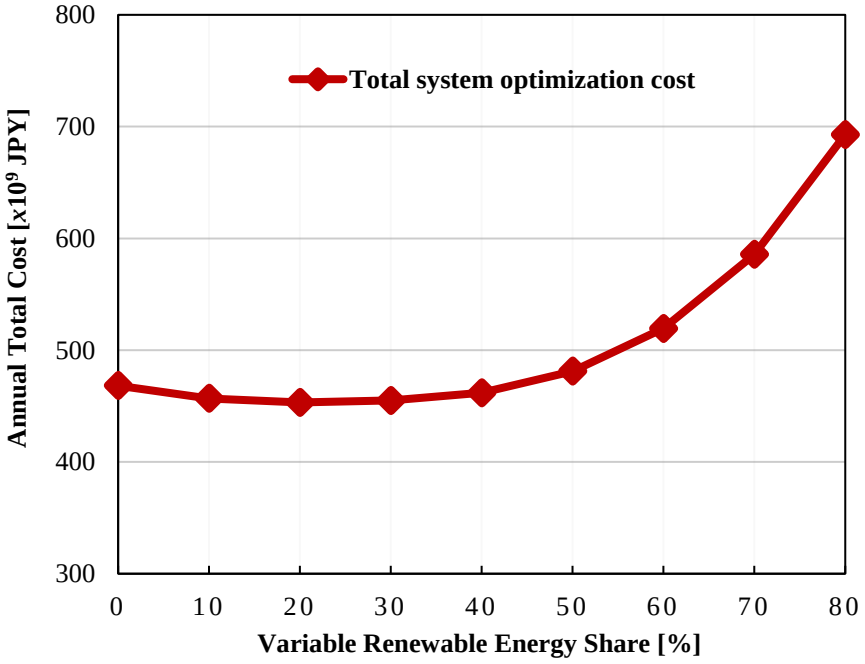

(a) Variation of Total annual power supply costs (JPY) by VRE share.

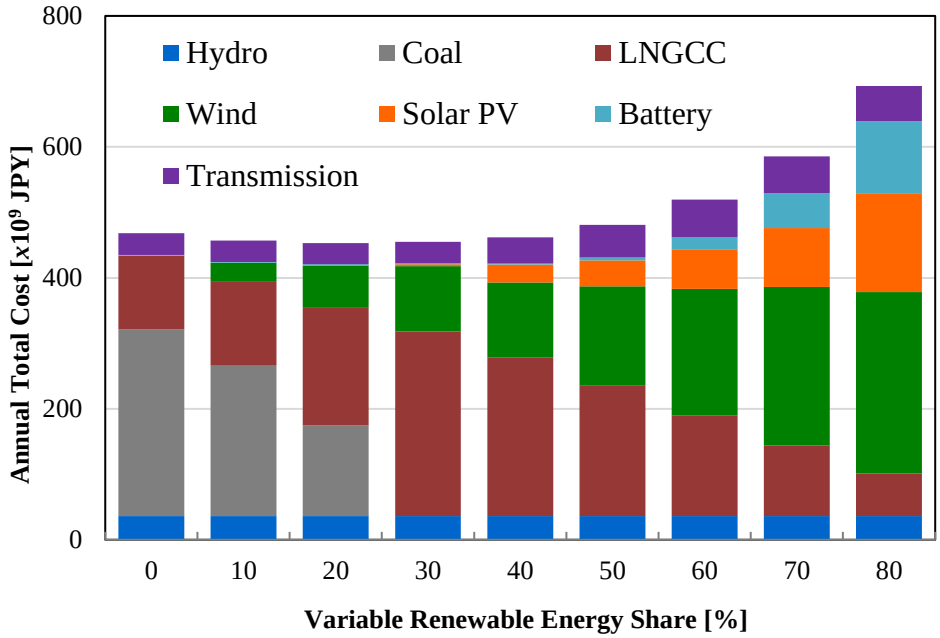

(b) Variation of the six components of the total annual power supply cost (JPY) by VRE share.

Fig. 4.2 Annual total cost of power supply. (a) Variation of Total annual power supply costs (JPY) by VRE share. (b) Variation of the six components of the total annual power supply cost (JPY) by VRE share.

Figure 4.3 shows the amount of power output and demand by VRE share for the total system optimization. The excess power output mainly from wind and solar PV is represented by the amount of power output above the power demand (black dotted line in Fig. 4.3). With higher VRE shares (40 ~ 80 %), the VRE power output fluctuations cause an increase in excess power output, which raises the power supply cost in Fig. 4.2 (a) with the increase in battery storage and transmission costs. The installed capacity for power generation, storage, and transmission at the 80% VRE share is shown in Fig. 4.4. The LNGCC is limited to the central region in this model while VRE is distributed such that wind power capacity is largest in the northern region which has a high wind power capacity factor. Simultaneously, the capacity of Central-North transmission, which is shown in the northern region in Fig. 4.4, is increased from the initial 0.4 GW (Fig. 2.2 (a)) to 1.86 GW to transmit the excess wind power output from the northern to the central region. Solar PV installations in the central region are the largest as the region has the largest electricity demand and high solar power capacity factors. The wind and solar power installed capacities in Fig. 4.4 are the baseline for the partial optimization analysis discussed in section 4.3.2. Further, the levelized cost of electricity (LCOE) for each power

generation component can be calculated from the annual cost of power generation (Fig. 4.3 (b)) divided by the amount of power output (Fig. 4.3). The LCOE varies depending on the capacity factor, and at the 80 % VRE share the LCOE is determined as 11 JPY/kWh for hydro, 19 JPY/kWh for LNGCC, 10 JPY/kWh for Wind, and 13 JPY/kWh for solar PV. These values are referred to when setting the price of electricity in the partial optimization analysis (section 4.3.2).

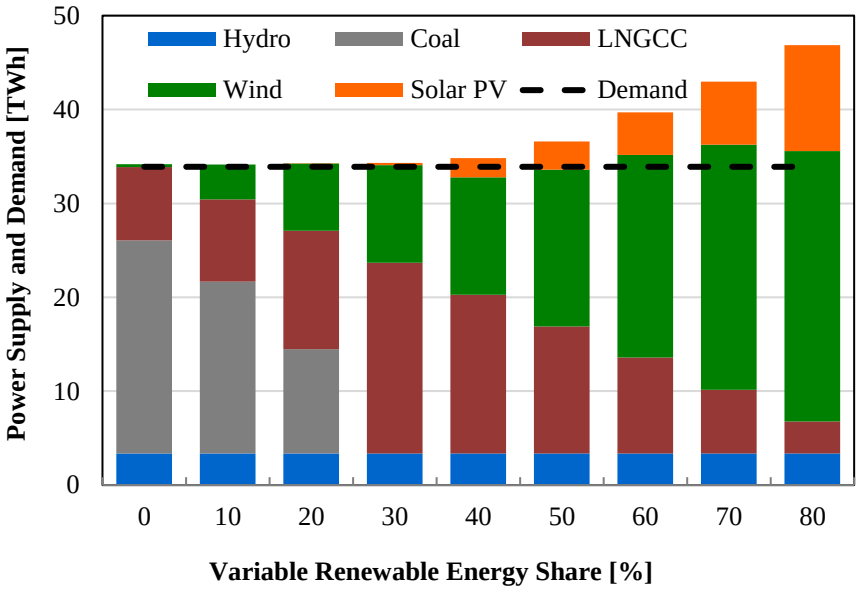

Fig. 4.3. Power supply components (TWh) and power demand (TWh) by Case and VRE share.

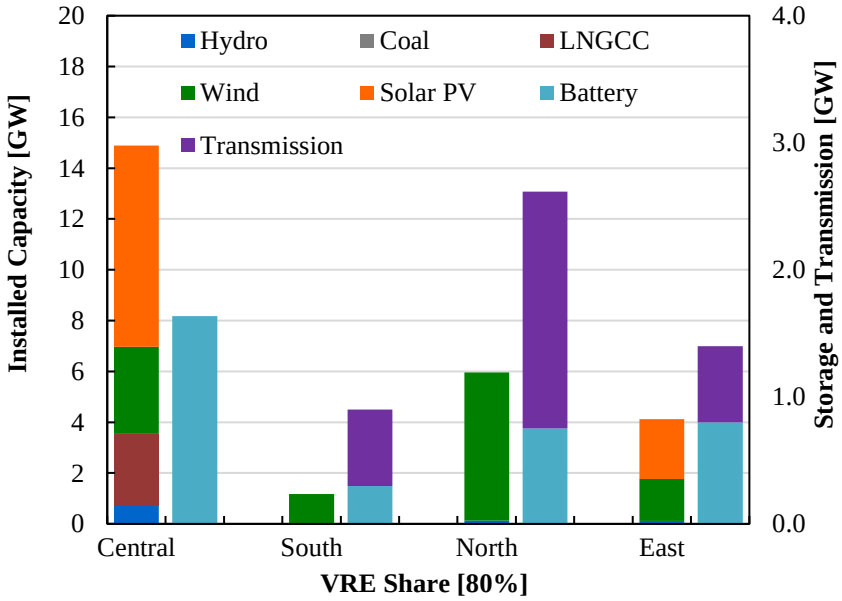

Fig. 4.4. Installed capacity of power supply, storage, and transmission at 80 % VRE share.

4.3.2 PTD company partial optimization

Under partial system optimization analysis, installed capacities of hydro, coal, wind, and solar PV in each region are fixed as shown in Fig. 4.4. The capacities of LNGCC, battery, and transmission are not fixed but optimized in the model to minimize the cost for the PTD company. Several price sets of electricity for power supply are considered in the analysis for discussion purposes, four price set scenarios, namely, P1, P2, P3, and P4, are presented here. The electricity price refers to the wholesale price at which the PTD company purchases power from the power generation companies. This study considers a future power supply system with high VRE shares and LNGCC electricity is used as backup power due to VRE power fluctuations. Therefore, to increase the VRE share and to evaluate the value of LNGCC backup electricity, the price of LNGCC electricity is varied in each price set scenario while the VRE electricity prices are kept constant. In P1, the price of electricity from LNGCC is 14 JPY/kWh, P2 is 37 JPY/kWh, P3 is 67 JPY/kWh, and P4 is 79 JPY/kWh. The renewable energy electricity prices are kept constant at 12 JPY/kWh for hydro, and 13 JPY/kWh for solar and wind in P1, P2, P3, and P4.

Figure 4.5 (a) shows the annual total power supply cost determined by the partial optimization model: four plots are for scenarios P1, P2, P3, and P4. The red line is the annual cost of power supply obtained from the total system optimization model (Fig. 4.2). The results show that the VRE share of electricity supply depends on the electricity prices; here the result of scenario P3 is the closest to that of the total system optimization. A decrease in the LNGCC electricity price increases the amount of LNGCC electricity and decreases the VRE share. In the P1 scenario, the total annual power supply cost is 656 billion JPY, with a VRE share of 60 %. This is 26 % higher than the total system optimization annual power supply cost of 519 billion JPY at 60 % VRE share. In this study, this difference in the total annual power supply cost is referred to as the additional cost of partial optimization. The cost of power generation from VRE is the same as that with the 80 % VRE share in the total system optimization, but the VRE share in P1 is only 60 %. Therefore, the additional cost is caused by the lower utilization of VRE installed capacity by the total system optimization for the 80 % VRE share. In scenarios P2 and P3, it is observed that the additional cost decreases with an increase in the LNGCC electricity price, while the additional cost increases slightly in scenario P4. In the P3 scenario, the additional cost is very minimal and the VRE share obtained is 80 %, which is similar to that of the total system optimization.

Figure 4.5(b) shows components of the power supply cost by VRE shares for the total system

optimization model (T) and partial system optimization model (P). The wind and solar PV capacities are fixed to the values in Fig. 4.4, and the VRE power supply cost is the same in all scenarios of the partial optimization (P). In the total optimization (T), each component of power supply cost is optimized at each VRE share, as in Fig. 4.2 (b). For the 60 % VRE share, the LNGCC costs are similar in both cases while the VRE power supply cost in the partial optimization model (P1) is higher than in the total optimization model (T1). This is because the VRE installed capacity in T1 is optimized in the total optimization model and becomes smaller than the fixed capacities in P1. Instead, the costs for battery storage and transmission in T1 are higher than in P1 to utilize the VRE power output. As a result, the total cost of power supply in partial optimization is higher than in total optimization. The partial optimization in P1 cannot utilize the VRE power suitable for an 80 % VRE share. As the LNGCC price becomes higher, the difference in the costs between total and partial optimizations becomes smaller, and for scenarios P3 and T3 with the 80 % VRE share, the total power supply costs are similar. This shows that a low wholesale price for the VRE electricity and a very high wholesale price for the LNGCC electricity (here, 13 JPY/kWh and 67 JPY/kWh, respectively) are needed for the utilization of the VRE installed capacity for the 80 VRE share. With the further high LNGCC price in P4, the total cost is slightly higher than in T4 with the same VRE share, 81 %, due to the overutilization of VRE electricity.

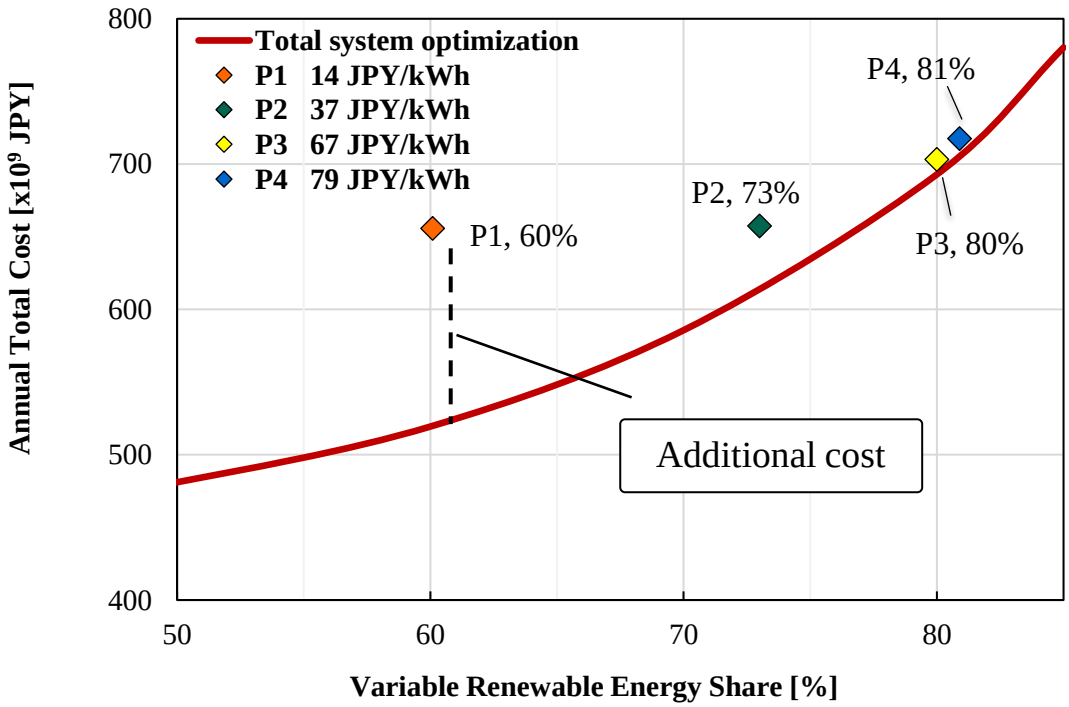

(a) Annual power supply cost.

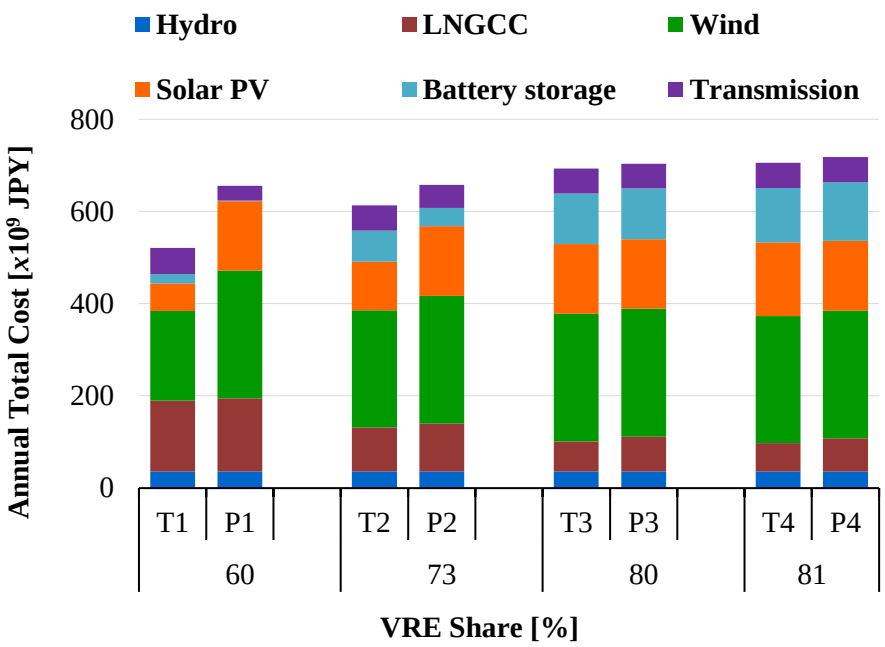

(b) Components of the power supply cost.

Fig. 4.5. Annual power supply cost for a power supply system under total optimization (T) and partial optimization (P). (a) Annual power supply cost. (b) Components of the power supply cost.

The components of (a) the total costs for PTD company and (b) the amounts of electricity purchased from power producers or input to battery storage and transmission line are shown in Fig. 4.6. The minimized cost of the PTD company increases with an increase in the price of LNGCC electricity as shown in Fig. 4.6 (a). In P1, the cost of battery storage is not significant and the PTD company supplies the electricity from geographically distributed VRE power producers without the storage to the power demand with a VRE share of 60 %. As the LNGCC price increases (P2, P3, and P4), the amount of electricity purchased from wind and solar PV increases in Fig. 4.6 (b) instead of LNGCC due to higher electricity price, and the VRE share increases (73, 80, 81 %, as shown in Fig. 4.5). Here, to utilize the VRE electricity, the amount of electricity input to battery storage and transmission line also increases. In P3, about 25 % of electricity is transmitted between regions. Further, about 15 % of electricity purchased is momentarily stored in batteries before being utilized to meet the power demand. The cost of LNGCC electricity also increases despite a decrease in the purchased amount. Then, the total cost for the PTD company increases, as in Fig. 4.6 (a). Figure 4.6 suggests that a high price of LNGCC is necessary to increase the share of VRE electricity and this increases the cost for the PTD company.

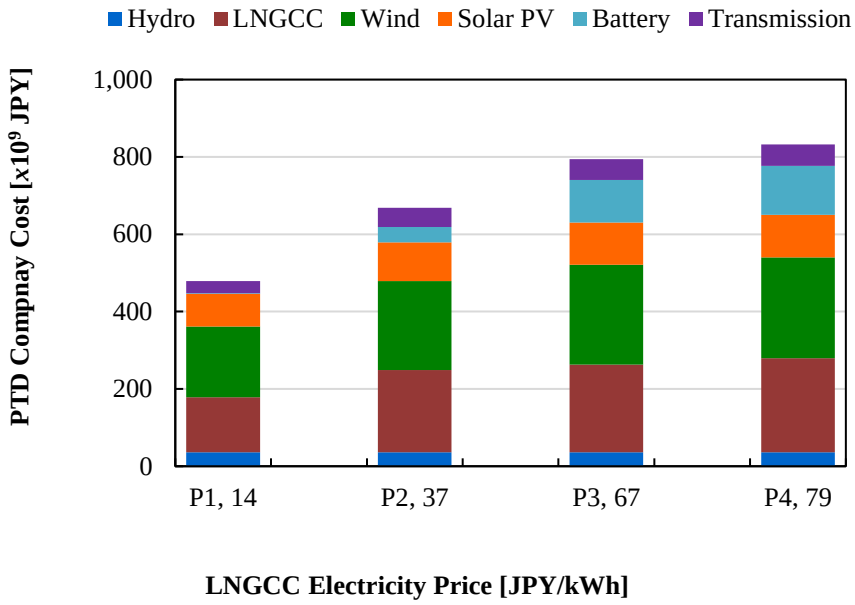

(a) Total cost of purchasing electricity and operating the battery and transmission systems.

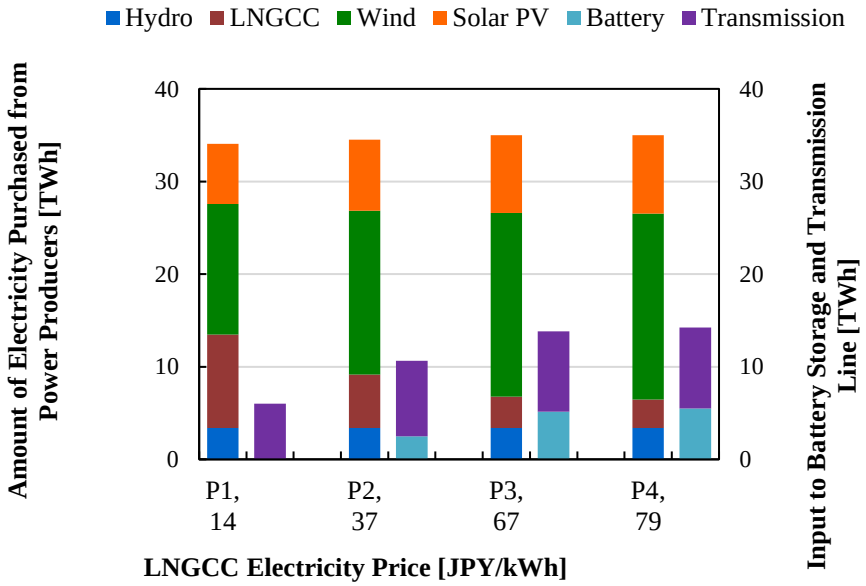

(b) Amount of electricity purchased from power producers (hydro, LNGCC, wind, and Solar

Fig. 4.6. PTD company cost, and the amount of power purchased. (a) The total cost of purchasing electricity from power producers and operating the battery and transmission systems. (b) Amount of electricity purchased from power producers (hydro, LNGCC, wind, and Solar PV) and input to battery storage and transmission line.

Figure 4.7 shows the hourly power output and demand profiles in the central (geographical) region for scenarios P1 and P3 in January on an hourly interval. In this figure, the power supply mix for 1 month can be observed. The P1 scenario consists of mainly local power supply from hydro, LNGCC, wind, and solar PV, with some amount of electricity transmitted in from the other regions. There is no battery storage installation, and the VRE electricity in the central region is supplied directly to the power demand. Surplus electricity is sometimes transmitted out to other regions mainly from LNGCC backup power for the VRE power fluctuations, backup LNGCC is only installed in the central region. In P3 (Fig. 4.7 (b), the amount of LNGCC decreases, and the amounts of power transmitted into the central region from other regions and discharged from battery storage increase. The increase in LNGCC price causes the LNGCC electricity to be replaced with electricity from battery discharge and power transmitted in from other regions with higher costs for VRE utilization.

(a) P1

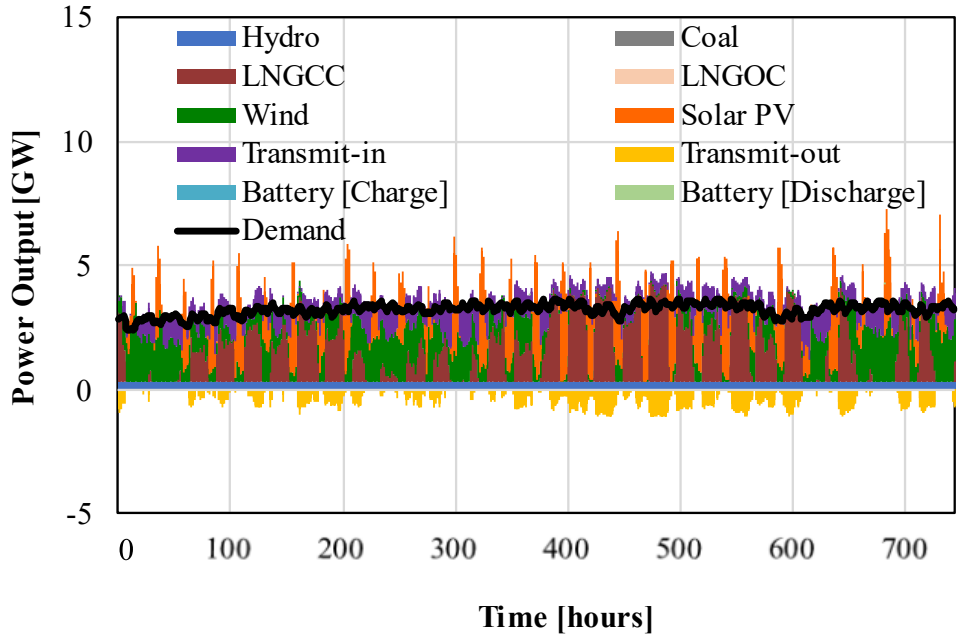

(b) P3

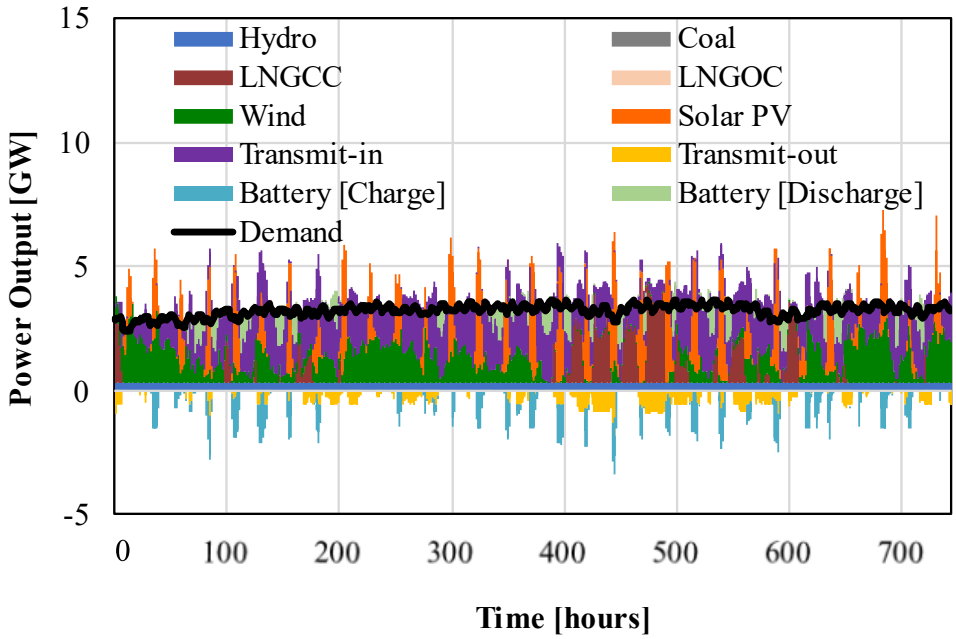

Fig. 4.7. Power output profile in the central region for January on an hourly interval at 80 % VRE share for (a) P1 and (b) P3 electricity price sets.

The results discussed above (Figs. 4.5 and 4.6) indicate that the electricity price difference between LNGCC and VRE is a key factor in the amount of VRE electricity purchased by the PTD company. To verify this observation, several electricity pricing scenarios with varying price differences are considered next. Figure 4.8 shows the wholesale electricity prices and the VRE share in the electricity supply mix. The A1~A12 are different sets of electricity price scenarios considered in the analysis. The price scenarios A1~A3, A4~A6, A7~A9, and A10~A12 show a price difference of 1, 24, 54, and 66 JPY/kWh, and A1, A4, A7, and A10, are equivalent to P1, P2, P3, and P4, respectively. The results in Fig. 4.8 show that electricity fee scenarios with the same price difference have the same VRE share. The VRE shares are 60, 73, 80, and 81 %, as in Fig. 4.5. The other parameters such as total power supply costs, power output profiles, and additional costs are consistent with those discussed in Figs. 4.5 to 4.7. These results show that the price difference between the VRE and the LNGCC electricity prices is a key factor for the PTD company to determine the VRE utilization.

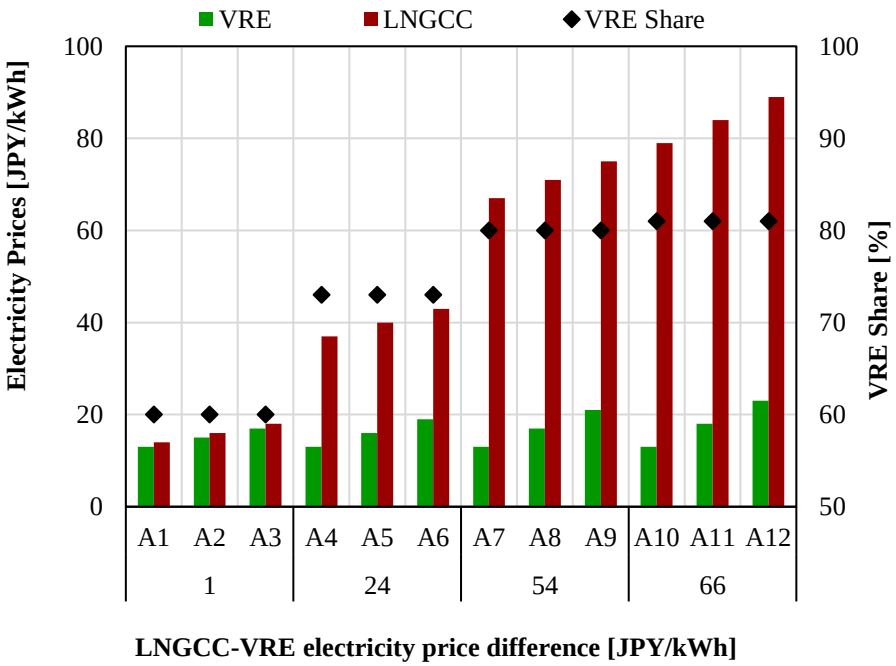

Fig. 4.8. Sets of electricity prices for hydro, VRE, and LNGCC electricity, and the resulting VRE share for a power supply system.

Figure 4.9 (a) shows the variations in the VRE share and the electricity price differences for the PTD company. The figure also shows the variation between the additional cost and the electricity price differences. The VRE share increases and the additional cost decreases with an increase in the electricity price difference, as in Fig. 4.5 (a). This is because of an increase in the utilization rate of VRE installed capacity. The additional cost at the 80 % VRE share is the minimum and is reduced to about 1.5 % of the power supply cost in the total optimization, 693 billion JPY. The large price difference enables the PTD company to opt for cheaper VRE electricity: a price difference of 54 JPY/kWh achieves the 80 % VRE share equivalent to the installed capacity. However, the rate of increase in the VRE share is high from 6 JPY/kWh to 30 JPY/kWh price difference. Above the 30 JPY/kWh price difference, the increase in the price difference does not yield significant increases in the VRE share. The 30 JPY/kWh price difference yields a 76% VRE share, which is only 4% less than the installed capacity of the 80 % VRE share. To further increase the VRE share to 80 %, an additional 24 JPY/kWh is needed which only adds 4 % to the 76 % obtained with a 30 JPY/kWh price difference. Therefore, a lower 30 JPY/kWh price difference giving a 76 % VRE share is more economical than the 54 JPY/kWh for an 80 % VRE share.

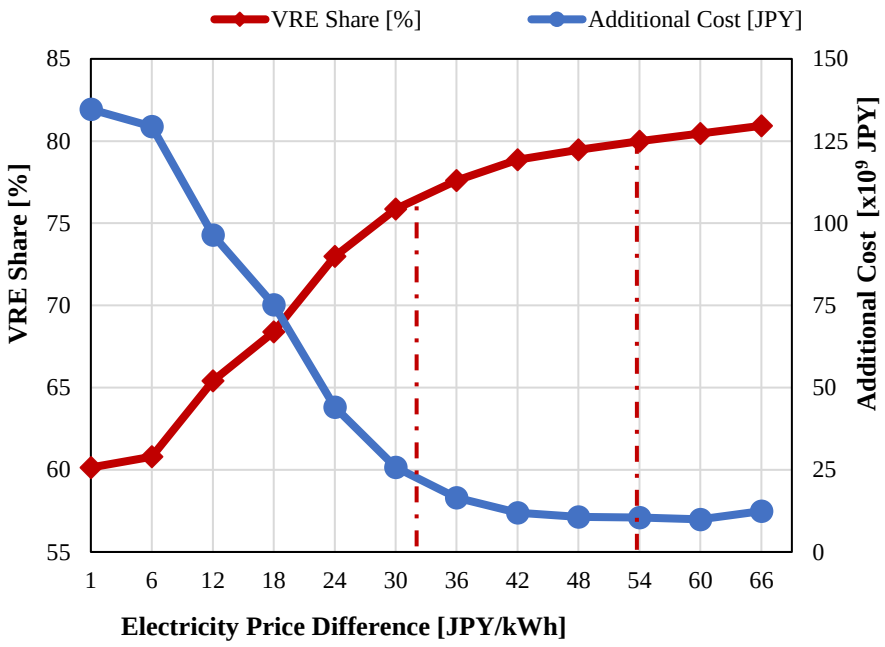

(a) Power supply installed capacity system with 80 % VRE share

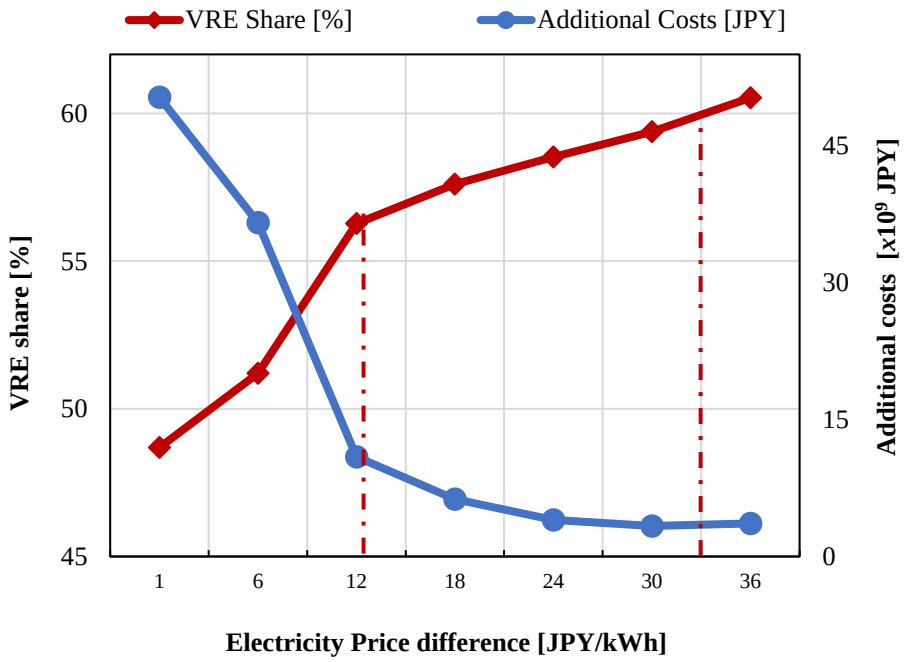

(b) Power supply installed capacity system with 60 % VRE share.

Fig. 4.9. Variation of VRE share and additional cost of VRE power purchase with the thermal and VRE power price difference. (a) Power supply installed capacity system with 80 % VRE share, and (b) Power supply installed capacity system with 60 % VRE share.

However, while the focus is on an ambitiously high target of 80 % optimum VRE share, it is worth considering the variation of VRE shares with electricity prices for a lower target of an optimum VRE share. Therefore, a similar analysis is applied to a partial system optimization of the PTD company with the target of a 60 % VRE share. In this case, the installed capacities of hydro, coal, wind, and solar PV in each region are fixed according to the results of the total system optimization at the 60 % VRE share. Figure 4.9 (b) illustrates the variation between the VRE share and price difference. Here, to achieve the target 60 % VRE share, an LNGCC electricity price of 46 JPY/kWh is necessary, representing a price difference of 33 JPY/kWh. However, a relatively lower price difference of 12 JPY/kWh yields a 56 % VRE share. Comparing Figs. 4.9 (a) and 4.9 (b) shows that for the PTD company to achieve an optimum VRE share of 80% and 60 %, the necessary price differences are 54 JPY/kWh and 33 JPY/kWh, respectively. At these price differences, the VRE share is equal to the optimum VRE share and the additional cost is minimum. Considering the rate of increase in the VRE share, a relatively lower price difference of 30 JPY/kWh and 12 JPY/kWh results in 76 % and 56 %, respectively. For higher VRE shares (80 %), a larger price difference is necessary because the PTD company needs to install battery storage and transmission systems. For a lower optimum VRE share (<<60%), a very low electricity price difference will be sufficient to obtain VRE electricity from VRE power producers by the PTD company. This is because lower VRE shares do not require very large battery storage and transmission capacities.

Further, with the 80 % VRE share and to discuss how the electricity price difference determines the VRE share in Fig. 4.8 and the effects in Fig. 4.9 (a), the relationship between the VRE power supply amount and the total cost for the PTD company is shown in Fig. 410. The twelve VRE supply amounts correspond to the results in Fig. 4.9 (a): 20.6 TWh supply is with 1 JPY/kWh and 28.5 TWh supply is with 66 JPY/kWh. The total cost to the PTD company consists of power purchase, battery storage, and transmission, so the difference between the total cost and the VRE power purchase cost in Fig. 4.10 equals the cost for battery storage and transmission by the PTD company. The gradient of the total cost is also shown in Fig. 4.10, as will be discussed later. When the amount of VRE power purchase is small (P1), the PTD company can transmit the VRE power directly to the power demand without the need for battery storage facilities. At the low VRE share, the PTD company cost is mainly comprised of the power purchase cost and the cost of installing the power transmission lines. However, with an increase in VRE power purchase, the effects of VRE power output fluctuations become more pronounced which increases the battery storage and transmission capacities to smoothen the VRE power output. This increase in the battery storage and transmission capacities causes an increase in the total cost to the

PTD company. While the VRE power purchase cost increase is nearly linear with a VRE electricity price of 13 JPY/kWh in Fig. 4.10, the increase in the total cost of the PTD company is non-linear. This is because the capacity factors of the increased battery storage and transmission lines become lower at higher VRE shares. The gradient expresses the unit cost for adding VRE electricity supply instead of the LNGCC electricity and could correspond to the necessary LNGCC electricity price for reducing the LNGCC electricity. At the lower VRE share of around 60 % (20.6 TWh VRE power purchase), the gradient is suppressed to about 20 JPY/kWh. This value corresponds to the LNGCC electricity price and a price difference between the LNGCC and VRE electricity of about 7 JPY/kWh. For P2 and P3, the total VRE power purchase amounts are 25.4 and 28.2 TWh, with the LNGCC electricity prices of 37 and 67 JPY/kWh, respectively. These LNGCC electricity prices correspond to the cost gradient in Fig. 4.10 and considering the rate of increase in the PTD company cost shows how the electricity price difference determines the VRE share, and a necessary price difference can be determined.

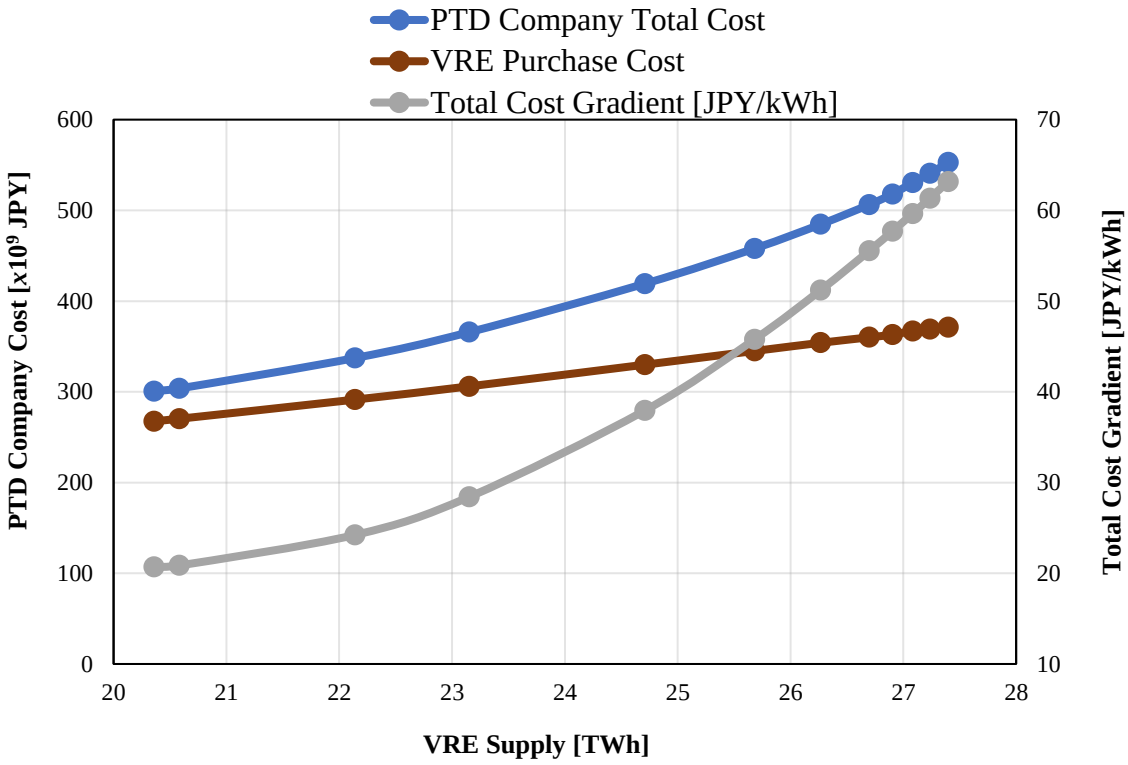

Fig. 4.10. Relationship between VRE power supply amount [TWh] and the power purchase, battery storage, and transmission cost [JPY]

In the partial optimization system of this study, the higher share of VRE power supply requires

higher prices of LNGCC electricity, resulting in a higher cost for the PTD company, as shown in Fig. 4.6 (a). This is because the higher shares of VRE require increases in battery storage and transmission line capacities to minimize the VRE power output fluctuations, as in Fig.4.10. It is also confirmed in Fig. 4.6 (a) that the power purchase costs for LNGCC and VRE also increase in addition to the increase in the storage and transmission costs. This means that the revenues of LNGCC and VRE power generation companies increase with the higher VRE share. The burden on the PTD company to increase the battery storage and transmission capacity due to higher VRE shares and reduction in CO2 emissions needs to be covered by all of the components of the power supply. Therefore, additional measures such as a carbon tax, cheaper prices of VRE electricity when it cannot be used directly, and subsidies to the PTD company may be effective to incentivize the installation of battery storage and transmission line systems. It may be concluded that the analysis using total and partial optimization in this study is a useful tool to evaluate effective measures for increasing the VRE share. .

4.4 Conclusions of chapter 4

This study considers the development of a method that combines total and partial system optimization of a power supply system. The power transmission and distribution component of the power supply system is the target of the partial optimization analysis. The partial optimization model is developed to determine the effective electricity price conditions necessary to optimize the utilization of VRE electricity of already installed VRE power generation systems. The combined model approach is applied to the power supply system of Hokkaido, and the effect of electricity prices from power generation companies on the utilization of VRE electricity is considered. From the results, it is concluded that:

- The VRE share of the electricity supply depends on the electricity prices. Lower prices of backup thermal power cause an increase in thermal power electricity and a decrease in the use of VRE electricity. The underutilization of VRE installed capacity gives rise to the additional cost of partial optimization. Higher prices of backup thermal power cause an increase in VRE utilization.

- The price difference between the VRE and the backup thermal power prices is a key factor in determining the VRE utilization by the PTD company. A larger price difference is necessary as it enables the PTD company to install additional energy storage and transmission systems,

which are necessary to increase the purchase of cheaper electricity from VRE sources. In the case study, for a power supply system with VRE installed capacities fixed at 80 % VRE share, a price difference of 54 JPY/kWh is necessary to obtain the 80 % VRE share by the PTD company. However, considering the rate of increase of the VRE share, a 30 JPY/kWh price difference is effective and obtains a 76 % VRE share, which is only 4 % below the optimum VRE share.

- Increasing the VRE share adds to the cost burden of installing energy storage and transmission systems by the PTD company. The additional energy storage and transmission facilities increase the cost of the PTD company. Instead of high electricity prices of backup thermal power, this burden on the PTD company needs to be covered by all components of the power supply system. Therefore, additional measures such as a carbon tax, cheaper VRE electricity prices, and subsidies to the PTD company may be effective to incentivize the installation of energy storage and transmission facilities.

5 Conclusions

In this research, the separate and combined effect of the geographical distribution of VRE locations, enhancements of power transmission capacity, and the introduction of battery storage on the integration of high VRE shares in the power supply system are considered. The analysis is applied to Hokkaido as a case study. From the results, it is concluded that;

- The combination of the geographical distribution of VRE locations, transmission capacity enhancement, and the introduction of battery storage, is the most economical way of integrating VRE in power supply systems. The effects of the combination of these three measures on the reduction of excess power generation and the reduction in the power supply costs outweigh that of individual effects or that of a combination of only two of these measures. To effectively increase the VRE share in a power supply system, careful consideration should be made for the geographical location of VRE sites and provisions should be made to upgrade the transmission capacity and introduce battery storage.

- To identify the combination of power fluctuation reduction measures effective to achieve a particular share of VRE in the power supply system, this study reveals that by geographically distributing the locations of VRE sites, up to 40 % VRE share can be achieved without upgrades to the power transmission and storage capacities. Therefore, it is important to optimize the location of solar and wind power generation sites through the selection of suitable sites from candidate sites. For the second tier of VRE share (40 % to 60 %), an increase in the transmission capacity coupled with VRE geographical distribution is needed to minimize the excess power generation and the total power supply cost. For VRE from 60 % to 80 %, the introduction of battery storage in addition to enhancements in transmission capacity provides an effective option for reducing excess power generation and minimizing the cost of power supply.

- The introduction of battery storage facilitates the integration of a larger capacity of solar PV power while transmission enhancement enables the integration of larger capacities of wind power.

- Applying the measures above still leaves a level of excess power generation increasing from the 60 % VRE share. However, excess power has potential applications in other sectors such as charging electric vehicles (EV) and hydrogen production for hydrogen-driven vehicles in the

transport sector. While these applications can significantly reduce the discarding of excess power, it is not certain if the discarding of power can be eliminated in power systems with high VRE shares. Further, the HVDC interconnection with the Honshu region also provides an avenue for the transmission of excess power from Hokkaido to the Honshu region.

- Additionally, a thermal backup system such as combined heat and power (CHP) may be a suitable candidate to mitigate costs incurred by the fluctuations. For heat supply, a heat pump system utilizing surplus power can also be integrated. The system would have the potential to effectively utilization of surplus power due to the utilization of both electricity and heat for various applications such as space heating during winter.

Further, a partial optimization model is developed to evaluate the effects of wholesale electricity prices on the power purchased by the PTD company. The model is applied to power supply systems to determine the electricity pricing conditions to maximize the VRE share in the power. Using the model, the effective electricity pricing conditions can be used to optimize the integration of electricity from VRE sources by the PTD company.

Further, this research considers the development of a method that combines the total and partial system optimization of a power supply system. The power transmission and distribution component of the power supply system is the target of partial optimization. A partial optimization model is developed to determine the effective electricity price conditions necessary to optimize the utilization of VRE electricity of already installed VRE power generation systems. The combined model approach is applied to the power supply system of Hokkaido, and the effect of electricity prices from power generation companies on the utilization of VRE electricity is considered. From the results it is concluded that;

- The VRE share of the electricity supply depends on the electricity prices. Lower prices of backup thermal power cause an increase in thermal power electricity and a decrease in the use of VRE electricity. The underutilization of VRE installed capacity gives rise to the additional cost of partial optimization. Higher prices of backup thermal power cause an increase in VRE utilization.

- The price difference between the VRE and the backup thermal power prices is a key factor in determining the VRE utilization by the PTD company. A larger price difference is necessary as it

enables the PTD company to install additional energy storage and transmission systems, which are necessary to increase the purchase of cheaper electricity from VRE sources. In the case study, for a power supply system with VRE installed capacities fixed at 80 % VRE share, a price difference of 54 JPY/kWh is necessary to obtain the 80 % VRE share by the PTD company. However, considering the rate of increase of the VRE share, a 30 JPY/kWh price difference is effective and obtains a 76 % VRE share, which is only 4 % below the optimum VRE share.

- Increasing the VRE share adds to the cost burden of installing energy storage and transmission systems by the PTD company. The additional energy storage and transmission facilities increase the cost of the PTD company. Instead of high electricity prices of backup thermal power, this burden on the PTD company needs to be covered by all components of the power supply system. Therefore, additional measures such as a carbon tax, cheaper VRE electricity prices, and subsidies to the PTD company may be effective to incentivize the installation of energy storage and transmission facilities.

6 References

[1] BP. BP Statistical Review of World Energy 2022. [Online] London: BP Statistical Review of World Energy 2022:1–60.

[2] UNFCCC, The Paris Agreement 2016, online (available on https://unfccc.int/process-and-meetings/the-paris-agreement/the-paris-agreement) (accessed July 19, 2022).

[3] Gielen D, Boshell F, Saygin D, Bazilian MD, Wagner N, Gorini R. The role of renewable energy in the global energy transformation. Energy Strategy Reviews 2019. DOI:10.1016/j.esr.2019.01.006.

[4] Ueckerdt F, Hirth L, Luderer G, Edenhofer O. System LCOE: What are the costs of variable renewables? Energy 2013;63:61–75. https://doi.org/10.1016/j.energy.2013.10.072.

[5] Holttinen H, Meibom P, Orths A, Lange B, O'Malley M, Tande JO, et al. Impacts of large amounts of wind power on design and operation of power systems, results of IEA collaboration. Wind Energy 2011;14:179–92. DOI:10.1002/we.410.

[6] Hirth L. The market value of variable renewables. The effect of solar wind power variability on their relative price. Energy Econ 2013;38:218–36. DOI:10.1016/j.eneco.2013.02.004.

[7] Hirth L, Ueckerdt F, Edenhofer O. Integration costs revisited - An economic framework for wind and solar variability. Renew Energy 2015;74:925–39. DOI:10.1016/j.renene.2014.08.065.

[8] Pietzcker RC, Ueckerdt F, Carrara S, de Boer HS, Després J, Fujimori S, et al. System integration of wind and solar power in integrated assessment models: A cross-model evaluation of new approaches. Energy Econ 2017;64:583–99. DOI:10.1016/j.eneco.2016.11.018.

[9] IEA. World Energy Outlook 2016. Economic Outlook 2016; DOI:10.1111/j.1468-0319.1987.tb00425.x.

[10] Lukwesa B, Takahashi N, Suzuki K, Tabe Y, Chikahisa T. Analysis of effective measures for power fluctuation mitigation of geographically distributed wind and solar power. Mechanical Engineering Journal 2022;9:21–00154. DOI:10.1299/mej.21-00154.

[11] Becker S, Rodriguez RA, Andresen GB, Schramm S, Greiner M. Transmission grid extensions during the build-up of a fully renewable pan-European electricity supply. Energy 2014. DOI:10.1016/j.energy.2013.10.010.

[12] Dujardin J, Kahl A, Kruyt B, Bartlett S, Lehning M. Interplay between photovoltaic, wind energy, and storage hydropower in a fully renewable Switzerland. Energy 2017;135:513–25. DOI:10.1016/j.energy.2017.06.092.

[13] Obara S, Utsugi Y, Ito Y, Morel J, Okada M. A study on planning for interconnected renewable energy facilities in Hokkaido, Japan. Appl Energy 2015. DOI:10.1016/j.apenergy.2015.02.037.

[14] Žiger I, Božičević-Vrhovčak M, Šimić Z. Geographical Distribution of Wind Power Plants and Its Influence on Power System Availability—Case Study Croatia. Energy Sources, 2015. DOI:10.1080/15567036.2011.597282.

[15] Al-Ghussain L, Samu R, Taylan O, Fahrioglu M. Sizing renewable energy systems with energy storage systems in microgrids for maximum cost-efficient utilization of renewable energy resources. Sustain Cities Soc, 2020. DOI:10.1016/j.scs.2020.102059.

[16] Bistline J, Blanford G, Mai T, Merrick J. Modeling variable renewable energy and storage in the power sector. Energy Policy 2021. DOI:10.1016/j.enpol.2021.112424.

[17] Heide D, von Bremen L, Greiner M, Hoffmann C, Speckmann M, Bofinger S. Seasonal optimal mix of wind and solar power in a future, highly renewable Europe. Renew Energy 2010. DOI:10.1016/j.renene.2010.03.012.

[18] Girard R, Laquaine K, Kariniotakis G. Assessment of wind power predictability as a decision factor in the investment phase of wind farms. Appl Energy 2013 DOI:10.1016/j.apenergy.2012.06.064.

[19] Monforti F, Huld T, Bódis K, Vitali L, D'Isidoro M, Lacal-Arántegui R. Assessing complementarity of wind and solar resources for energy production in Italy. A Monte Carlo approach. Renew Energy 2014. DOI:10.1016/j.renene.2013.10.028.

[20] Østergaard PA. Modelling grid losses and the geographic distribution of electricity generation. Renew Energy 2005. DOI:10.1016/J.RENENE.2004.09.007.

[21] Collins S, Deane P, Ó Gallachóir B, Pfenninger S, Staffell I. Impacts of Inter-annual Wind and Solar Variations on the European Power System. Joule 2018. DOI:10.1016/j.joule.2018.06.020.

[22] Okada M, Onishi T, Obara S. A design algorithm for an electric power system using wide-area interconnection of renewable energy. Energy 2020. DOI:10.1016/j.energy.2019.116638.

[23] Suzuki K, Nakanishi T, Tabe Y, Chikahisa T. Optimizing geographical distribution of wind power plants in Hokkaido to minimize power reduction risk. Transactions of the JSME (in Japanese) 2014. DOI:10.1299/transjsme.2014tep0092.

[24] Geth F, Brijs T, Kathan J, Driesen J, Belmans R. An overview of large-scale stationary electricity storage plants in Europe: Current status and new developments. Renewable and Sustainable Energy Reviews 2015. DOI:10.1016/j.rser.2015.07.145.

[25] Ibrahim H, Ilinca A, Perron J. Energy storage systems-Characteristics and comparisons. Renewable and Sustainable Energy Reviews 2008. DOI:10.1016/j.rser.2007.01.023.

[26] Divya KC, Østergaard J. Battery energy storage technology for power systems-An overview. Electric Power Systems Research 2009. DOI:10.1016/j.epsr.2008.09.017.

[27] Ferreira HL, Garde R, Fulli G, Kling W, Lopes JP. Characterisation of electrical energy storage technologies. Energy 2013. DOI:10.1016/j.energy.2013.02.037.

[28] Liao Q, Sun B, Liu Y, Sun J, Zhou G. A techno-economic analysis on NaS battery energy storage system supporting peak shaving. Int J Energy Res 2016. DOI:10.1002/er.3460.

[29] Zakeri B, Syri S. Electrical energy storage systems: A comparative life cycle cost analysis. Renewable and Sustainable Energy Reviews 2015. DOI:10.1016/j.rser.2014.10.011.

[30] Kimura K. Feed-in Tariffs in Japan: Five Years of Achievements and Future Challenges. 2017.

[31] Edahiro J. Current Status of Renewable Energy in Japan. Japan for Sustainability 2017. https://www.japanfs.org/sp/en/news/archives/news_id035824.html (accessed August 30, 2021).

[32] Japan Meteorological Business Support Center (JMBSC). Hourly and daily data of terrestrial observatories in 2014 2019. http://www.jmbsc.or.jp/en/meteo-data.html.

[33] Standards JI. Estimation Method of Generating Electric Energy by PV Power System JIS C 8907 (2005). 2005.

[34] Carrillo C, Obando Montaño AF, Cidrás J, Díaz-Dorado E. Review of power curve modelling for wind turbines. Renewable and Sustainable Energy Reviews 2013. DOI:10.1016/J.RSER.2013.01.012.

[35] Hokkaido Electric Power Co. Inc. Power supply configuration / Equipment Data 2021. http://www.hepco.co.jp/corporate/company/ele_power.html (accessed September 1, 2021).

[36] Esteban M, Portugal-Pereira J, Mclellan BC, Bricker J, Farzaneh H, Djalilova N, et al. 100% renewable energy system in Japan: Smoothening and ancillary services. Appl Energy 2018. DOI:10.1016/j.apenergy.2018.04.067.

[37] Hokkaido Electric Power Co. Inc. Hokkaido Electric Power Co. Ltd. Past Power Usage Data (2014) 2014. https://denkiyoho.hepco.co.jp/area_download.html (accessed September 30, 2018).

[38] Hokkaido Electric Power Network Co. L. Supply and demand performance in the Hokkaido area (2020). https://www.hepco.co.jp/network/renewable_energy/fixedprice_purchase/supply_demand_results.html (accessed August 31, 2021).

[39] Ministry of Economy, Trade and Industry (METI). Japan's Energy 2020, online (accessed November 1, 2021) available on https://www.enecho.meti.go.jp/en/category/brochures/pdf/japan_energy_2020.pdf.

[40] International Energy Agency (IEA). Japan 2021 - Energy Policy Review. 2021.

[41] National Institute of Population and Social Security Research (NIPSSR). Population and Social Security in Japan. 2019.

[42] Ministry of Economy, Trade and Industry (METI), Power Generation Cost Verification Working Group: Power Generation Cost Review Sheet 2015 (accessed September 1, 2021). https://www.enecho.meti.go.jp/committee/council/basic_policy_subcommittee/mitoshi/cost_wg/xls/cost_wg_01.xls

[43] BP, Statistical Review of World Energy, (2020), online (accessed on 30 August 2021).

[44] Ford A. Global climate change and the electric power industry. Competitive Electricity Markets, Elsevier Ltd; 2008. DOI:10.1016/B978-008047172-3.50018-0.

[45] International Energy Agency (IEA). World Energy Outlook 2015 2015. DOI:doi.org/10.1787/weo-2015-en.

[46] Ueckerdt F, Brecha R, Luderer G. Analyzing major challenges of wind and solar variability in power systems. Renew Energy 2015. DOI:10.1016/j.renene.2015.03.002.

[47] Ito Y, Obara S. A study on installation planning for interconnected renewable energy facilities in Hokkaido, Japan. Asia-Pacific Power and Energy Engineering Conference, APPEEC 2016. DOI:10.1109/APPEEC.2016.7779754.

[48] Barasa M, Bogdanov D, Oyewo AS, Breyer C. A cost optimal resolution for Sub-Saharan Africa powered by 100% renewables in 2030. Renewable and Sustainable Energy Reviews 2018. DOI:10.1016/j.rser.2018.04.110.

[49] Aghahosseini A, Bogdanov D, Breyer C. Towards sustainable development in the MENA region: Analysing the feasibility of a 100% renewable electricity system in 2030. Energy Strategy Reviews 2020. DOI:10.1016/j.esr.2020.100466.

[50] de Barbosa LSNS, Bogdanov D, Vainikka P, Breyer C. Hydro, wind and solar power as a base for a 100% renewable energy supply for South and Central America. PLoS One 2017. DOI:10.1371/journal.pone.0173820.

[51] Schaber K, Steinke F, Hamacher T. Transmission grid extensions for the integration of variable renewable energies in Europe: Who benefits where? Energy Policy 2012. DOI:10.1016/j.enpol.2011.12.040.

[52] Shibata S, Komiyama R, Fujii Y, Generation WP, Line T, Power O, et al. Evaluation of the Optimal Power Generation Mix with Regional Power Interchange considering Output Fluctuation of Photovoltaic System and Wind Power Generation 2009.

[53] Nakayama S, Azuma H, Fukutome S, Ogimoto K. Analysis of value of flexibility in Japan's power system with increased VRE. Clean Energy 2018. DOI:10.1093/ce/zky005.

[54] Harasawa J, Ikegami T. Load leveling effects by massively introduced residential battery storage systems. 2017 IEEE Innovative Smart Grid Technologies - Asia: Smart Grid for Smart Community, ISGT-Asia 2017 2018. DOI:10.1109/ISGT-Asia.2017.8378386.

[55] Esteban M, Zhang Q, Utama A. Estimation of the energy storage requirement of a future 100% renewable energy system in Japan. Energy Policy 2012. DOI:10.1016/j.enpol.2012.03.078.

[56] Komiyama R, Shibata S, Fujii Y. Assessment of optimal power generation mix considering extensive variable renewable energy and nationwide power interchange through tie lines. Electrical Engineering in Japan 2014. DOI:10.1002/eej.22576.

[57] Steinke F, Wolfrum P, Hoffmann C. Grid vs. storage in a 100% renewable Europe. Renew Energy 2013. DOI:10.1016/j.renene.2012.07.044.

[58] Obara S, Ito Y, Okada M. Optimization algorithm for power-source arrangement that levels the fluctuations in wide-area networks of renewable energy. Energy 2018. DOI:10.1016/j.energy.2017.10.038.

[59] Wallenius T, Lehtomäki V. Overview of cold climate wind energy: Challenges, solutions, and future needs. Wiley Interdiscip Rev Energy Environ 2016. DOI:10.1002/wene.170.

[60] Akpinar EK, Akpinar S. An assessment on seasonal analysis of wind energy characteristics and wind turbine characteristics. Energy Convers Manag 2005. DOI:10.1016/j.enconman.2004.08.012.

[61] Pryor SC, Barthelmie RJ. Climate change impacts on wind energy: A review. Renewable and Sustainable Energy Reviews 2010. DOI:10.1016/j.rser.2009.07.028.

[62] Obara S, Utsugi Y, Ito Y, Morel J, Okada M. A study on planning for interconnected renewable energy facilities in Hokkaido, Japan. Appl Energy 2015. DOI:10.1016/j.apenergy.2015.02.037.

[63] IRENA (2022), Renewable Energy Statistics 2022, The International Renewable Energy Agency, Abu Dhabi.

[64] IRENA (2022), Renewable Power Generation Costs in 2021, International Renewable Energy Agency, Abu Dhabi.

[65] IEA. Global Energy Review 2020 2020. https://www.iea.org/reports/global-energy-review-2020 (accessed July 21, 2022).

[66] IEA. World Energy Outlook 2020 2020. https://www.iea.org/reports/world-energy-outlook-2020 (accessed July 21, 2022).

[67] Gielen D, Boshell F, Saygin D, Bazilian MD, Wagner N, Gorini R. The role of renewable energy in the global energy transformation. Energy Strategy Reviews 2019. DOI:10.1016/j.esr.2019.01.006.

[68] Sugiyama T, Komiyama R, Fujii Y. Optimal Power Generation Mix Model considering Nationwide High-voltage Power Grid in Japan for the Analysis of Large-scale Integration of PV and Wind Power Generation. IEEJ Transactions on Power and Energy 2016. DOI:10.1541/ieejpes.136.864.

[69] Laha P, Chakraborty B, Østergaard PA. Electricity system scenario development of India with import independence in 2030. Renew Energy 2020. DOI:10.1016/j.renene.2019.11.059.

[70] Sørensen B., Conditions for a 100% renewable energy supply system in Japan and South Korea,. International Journal of Green Energy, 2017. DOI:10.1080/15435075.2016.1175355.

Acknowledgements

Firstly, I would like to express my deepest gratitude and appreciation to my supervisor, Professor Yutaka Tabe, for his support and guidance in my research work and in my stay in Japan. I am grateful for giving me the opportunity to pursue the doctoral degree and conduct my research in the laboratory of energy conversion systems. I would also like to extend my gratitude and appreciation to Professor Suguru Uemura, Professor Takemi Chikahisa, and Professor Kengo Suzuki (University of Tsukuba) for their advice and contributions to my research work.

Further, I would like to extend my heartfelt appreciation to my wife, Dr. Mwangala A. Lukwesa, for her tremendous support throughout my studies and to my daughters, Joanne M. Lukwesa, and Isabel A. Lukwesa for always putting a smile on face. My wife and daughters have been a strong pillar of support throughout my studies and a motivation to put in more effort in my studies.

Above all, I am grateful to God for His abundance grace that saw me through to the successful completion of doctoral degree.

List of publications

1. Journal articles (related to doctoral thesis)

[1] Biness Lukwesa, Naoya Takahashi, Kengo Suzuki, Yutaka Tabe, Takemi Chikahisa, Analysis of effective measures for power fluctuation mitigation of geographically distributed wind and solar power, Mechanical Engineering Journal, 2022, DOI:10.1299/mej.21-00154.

[2] Biness Lukwesa, Suguru Uemura, Yutaka Tabe, Analysis of electricity prices for power supply toward a social optimum for wind and solar power utilization, Mechanical Engineering Journal, (submitted to Mech. Eng. Journal).

2. Journal articles (others)

[1] Randall Spalding-Fecher, Mamahloko Senatla, Francis Yamba, Biness Lukwesa, Grayson Himunzowa, Charles Heaps, Arthur Chapman, Gilberto Mahumane, Bernard Tembo, Imasiku Nyambe, Electricity supply and demand scenarios for the Southern African power pool, Energy Policy, 2017, DOI:10.1016/j.enpol.2016.10.033.

3. Academic conference proceedings (related to doctoral thesis)

[1] Biness Lukwesa, Wataru Sato, Yutaka Tabe, Takemi Chikahisa, "Leveling Technology of Grid Balance for Large-Scale Installation of Wind and Solar Power in Hokkaido", 33rd International Conference on Efficiency, Cost, Optimization, Simulation and Environmental Impact of Energy Systems (ECOS 2020), Osaka, June 29 - July 3, 2020.

[2] Biness Lukwesa, Suguru Uemura, Yutaka Tabe, Analysis of conditions for the power transmission and distribution company to select high shares of variable renewable energy and minimize the total social cost of power, Proceedings of the International Conference on Power Engineering (ICOPE), 2021, DOI:10.1299/jsmeicope.2021.15.2021-0169.

[3] Biness Lukwesa, Suguru Uemura, Yutaka Tabe, Analysis of electricity price effect on utilization of variable renewable energy electricity in the power supply mix, Proceedings of the Grand Renewable Energy International Conference (GRE 2022), Dec.13 - 20, 2022.

4. Academic conference proceedings (others)

[1] Biness Lukwesa, Yutaka Tabe, Takemi Chikahisa, Optimum option of selecting Energy Supply Infrastructures for Power Generation in Zambia, 56th Japan Society of Mechanical Engineers Hokkaido Branch Conference, 2018, DOI: 10.1299/jsmehokkaido.2018.56.432.

[2] Biness Lukwesa, Yutaka Tabe, Takemi Chikahisa, Optimization of Power Supply Systems with Large-scale Solar and Wind Energy in Zambia, Proceedings of Mechanical Engineering Congress, Japan, 2019, DOI: 10.1299/jsmemecj.2019.J05317P.

[3] Wataru Sato, Biness Lukwesa, Yutaka Tabe, Study on Mitigating Power Fluctuation of Variable Renewable Energy toward Reducing CO2 Emission in Hokkaido, Proceedings of Mechanical Engineering Congress, Japan, 2020, (in Japanese), DOI:10.1299/jsmemecj.2020.J05301.